

# We are IntechOpen, the world's leading publisher of Open Access books Built by scientists, for scientists

6,900

Open access books available

186,000

International authors and editors

200M

Downloads

Our authors are among the

154

Countries delivered to

TOP 1%

most cited scientists

12.2%

Contributors from top 500 universities



WEB OF SCIENCE™

Selection of our books indexed in the Book Citation Index  
in Web of Science™ Core Collection (BKCI)

Interested in publishing with us?  
Contact [book.department@intechopen.com](mailto:book.department@intechopen.com)

Numbers displayed above are based on latest data collected.  
For more information visit [www.intechopen.com](http://www.intechopen.com)



## Phosphate Rocks

Petr Ptáček

Additional information is available at the end of the chapter

<http://dx.doi.org/10.5772/62214>

### Abstract

Apatite is the most abundant phosphate mineral which include more than 95% of all phosphorus in the Earth's crust. The seventh chapter of this book provides brief description of sedimentary and igneous phosphate rocks and introduces basic ideas for characterization and classification of phosphate rocks. The chapter continues with description of biogenic apatites, description of phosphate rocks deposits and introduces other sources of phosphorus. Furthermore, geological role of apatite, cycle of phosphorus, weathering of apatite, fission track analysis and extraterrestrial apatites were described. The last section is dedicated to structure and properties important of non-apatitic phosphate minerals, such as atuanite, crandallite, lazulite, millisite, monazite, tobernite, xenotime etc.

**Keywords:** Apatite, Phosphate Rock, Biogenic Apatites, Fission Track, Extraterrestrial Apatite, Non-Apatitic Phosphate Minerals

Apatite [ $\text{Ca}_5(\text{PO}_4\text{CO}_3)_3(\text{OH},\text{F},\text{Cl})$ ] is the most abundant phosphate mineral, which accounts for more than 95% of all phosphorus in the Earth's crust and is found as an accessory mineral in most rock types on the Earth's surface, primarily because it is stable in a wide variety of geological conditions and over a range of different geological processes [1],[2],[3],[4],[5],[6],[7],[8]. According to the list of symbols for rock- and ore-forming minerals, the abbreviated symbol used for apatite is **Ap** [9].

However, exploitable deposits of apatite are mainly found in igneous rocks and also in sedimentary and metamorphic rocks. The former comprises the stratiform phosphorite deposits in shelf-type shale-carbonate sequences, which contain high phosphorus ores of microcrystal-

<sup>1</sup> A rock may be best defined as any mineral or aggregate of minerals that forms an essential part of the Earth [10]. Apatite is found in all classes of rock: igneous, metamorphic and sedimentary [2]. Also, much of phosphorus in coal is present in the form of apatite [7]. Phosphorus is the 10th most abundant element on Earth, with an average crustal abundance of 0.1% [8].

line CO<sub>2</sub>-rich fluorapatite (francolite) and cryptocrystalline collophane. The igneous deposits comprise fluorapatite ores, which mostly accommodate carbonatites and other types of alkaline intrusions. The magmatic ores are generally of lower grade but give higher-quality beneficiation products with low contents of unwanted contaminants (Cd, Pb, As, U, Th, Mg and Al) [11], [12].

The beneficiation products of apatite ores as a commodity are traded as phosphate rock. It is the only significant global resource of phosphorus used dominantly in the manufacturing of nitrogen-phosphorus-potassium (NPK) fertilizers for food-crop nutrition and in the production of animal feed supplements. Only 10 – 15% of the world’s production of phosphate rock has other applications (e.g. pharmaceuticals, ceramics, textiles and explosives) and represents an important alternative source of rare-earth elements (REE) [12],[13]. The REE contents in apatites are useful in paleoceanographic studies to identify the seawater masses and circulation patterns or to quantify the redox state of the ocean [14].

The composition of phosphate rocks varies from one deposit to another. Therefore, phosphate rocks from different sources may be expected to behave differently in beneficiation and acidulation processes. Phosphate rocks are primarily composed of the apatite group in association with a wide assortment of accessory minerals, mainly fluorides, carbonates, clays, quartz, silicates and metal oxides [13],[15],[16].

Si, Ca, Fe and Al are the most common companion elements in phosphate rocks, with the median abundances of 53.3 wt.%, 30.0 wt.%, 13.6 wt.% and 8.0 wt.%, respectively, compared

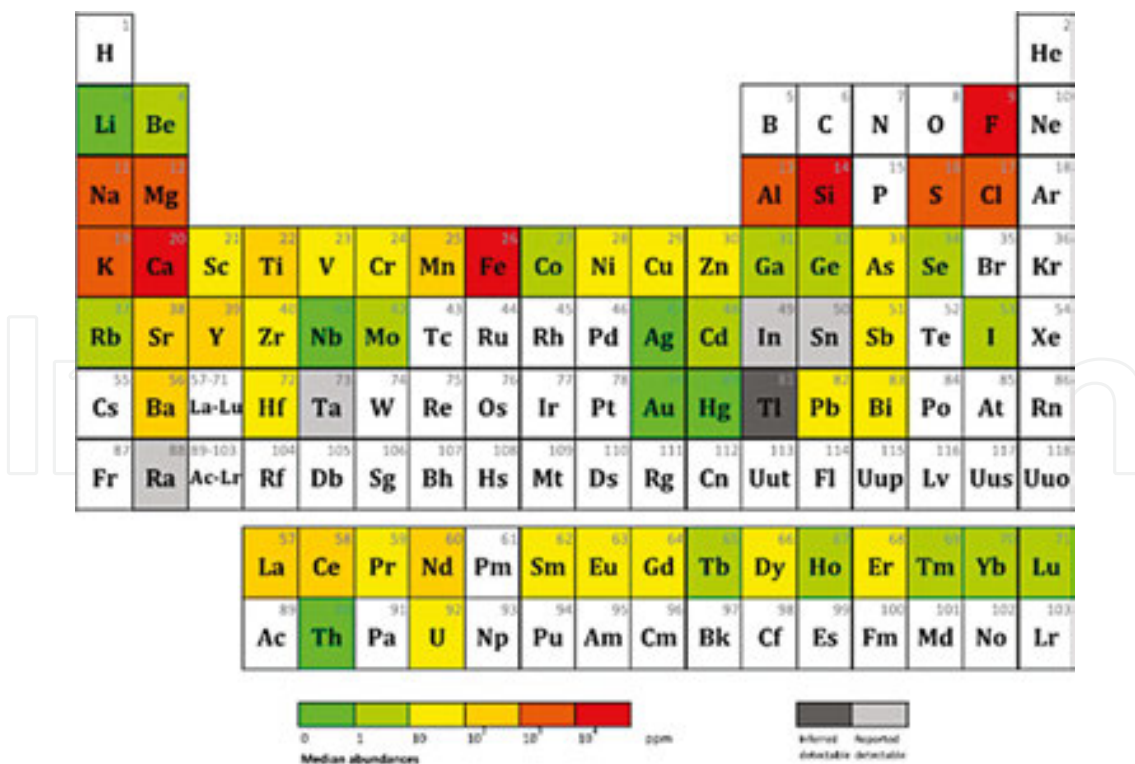


Fig. 1. The average distribution of trace elements in phosphate rock [17].

with  $P_2O_5$ . In some low-grade phosphate rock mines, the content of Fe and Al is even higher than that of  $P_2O_5$ , and it is usual that the  $P_2O_5$  content in phosphate rock is less than the Si and Ca content. In addition, some elements that are very rare in the Earth's crust are found to be relatively abundant (Fig. 1) in phosphate rocks [17].

## 7.1. Characterization and classification of phosphate rocks

When rock contains phosphate components between 5 and 50% (by volume), then it is phosphatic, and the name of the main lithology is used as a suffix (phosphatic limestone, phosphatic claystone, etc.). In addition, the dominant textural form of the phosphate components in a phosphorite can be used in defining the rock name (e.g. peloidal<sup>2</sup>) (phosphorite, coprolitic phosphorite, etc.) [10],[18].

There are two main kinds of phosphate rocks deposits in the world [10],[20],[21],[22],[17],[23]:

1. **Sedimentary phosphate rocks:** marine phosphate deposit, metamorphic deposit, biogenic deposit (bird and bat guano accumulation) and phosphate deposit as the result of weathering. The sedimentary deposits contain the varieties of carbonate-fluorapatite that are collectively called as francolite (Section 2.6). The most common non-phosphatic accessory minerals associated with sedimentary phosphate rocks are quartz, clay and carbonates (calcite and dolomite). Phosphate rocks of high concentration of phosphates (10 – 15% of  $P_2O_5$ ) are called phosphorites.
2. **Igneous phosphate rocks:** apatite is a common accessory mineral occurring in practically all types of igneous rocks (acid, basic or ultrabasic).

Depending on their origin (igneous or sedimentary), phosphate rocks have widely varying mineralogical, textural and chemical characteristics [23]. The locations of the major phosphate rocks deposit and producers are shown in Fig. 2 [20],[24].

Sedimentary phosphate deposits are exploited to produce about 80% of the total world production of phosphate rocks. Igneous phosphate deposits are often associated with carbonatites<sup>3</sup> and/or alkalic (silica-deficient) intrusions. Igneous phosphate rock concentrates are produced from the deposits mainly exploited in Russia, the Republic of South Africa, Brazil, Finland and Zimbabwe. Igneous phosphate ores are often low in grade (less than 5%  $P_2O_5$ ) but can be upgraded to high-grade products (from about 35% to over 40%  $P_2O_5$ ) [22],[23].

The atom ratio of P:N = 1:15(16) in the oceans is not greatly different from that found in living organisms. The availability of soluble phosphate from weathering of apatite-containing rocks may initially has been the rate-determining factor in early live development. In most ecolog-

<sup>2</sup> Peloid is a comprehensive descriptive term for polygenetic grains composed of micro- and polycrystalline carbonate. The term was proposed in order to replace the widely used name "pellet," which for many authors had become a synonym for pelletal coprolites (fossilized faces). Peloids differ from ooids and oncoids by the absence of centrosymmetric or radial internal structures [19].

<sup>3</sup> Igneous rocks (intrusive or extrusive) that contain carbonates in the amount higher than 50%.

ical systems, the phosphate content is the limiting factor for growth. Nearly all igneous rocks contain some phosphate, even if it is only ~0.1% (0.2%  $P_2O_5$  on average in lithosphere), with nearly all of it in the form of apatite. Sedimentary rocks generally contain rather less (~0.1%  $P_2O_5$  on average). Sedimentary phosphorite is believed to originate from widely dispersed apatite mainly in igneous rocks [25].

### 7.1.1. Sedimentary phosphate rocks

Most marine sediments and rocks contain less than 0.3% of  $P_2O_5$ . However, periodically through geological time, phosphorites (with the content of  $P_2O_5$  of 5% or greater) formed on the seafloor in response to specialized oceanic conditions and accumulated in sufficient concentrations to produce major deposits of regional extent<sup>4</sup> [26].

Marine phosphate formation and deposition represent the periods of low rates of sedimentation in combination with large supplies of nutrients. Phosphorus is then concentrated by various mechanisms, possibly bacterial (refer to discussion of Fig. 7), at either the sediment-water interface or within interstitial pore waters. This process leads to primary formation and growth of phosphate grains, which remain where they were formed or are transported as clastic particles within the environment of formation. During subsequent periods of time, some primary phosphate grains may be physically reworked into another sediment unit in response to either changing or different environmental processes [26].

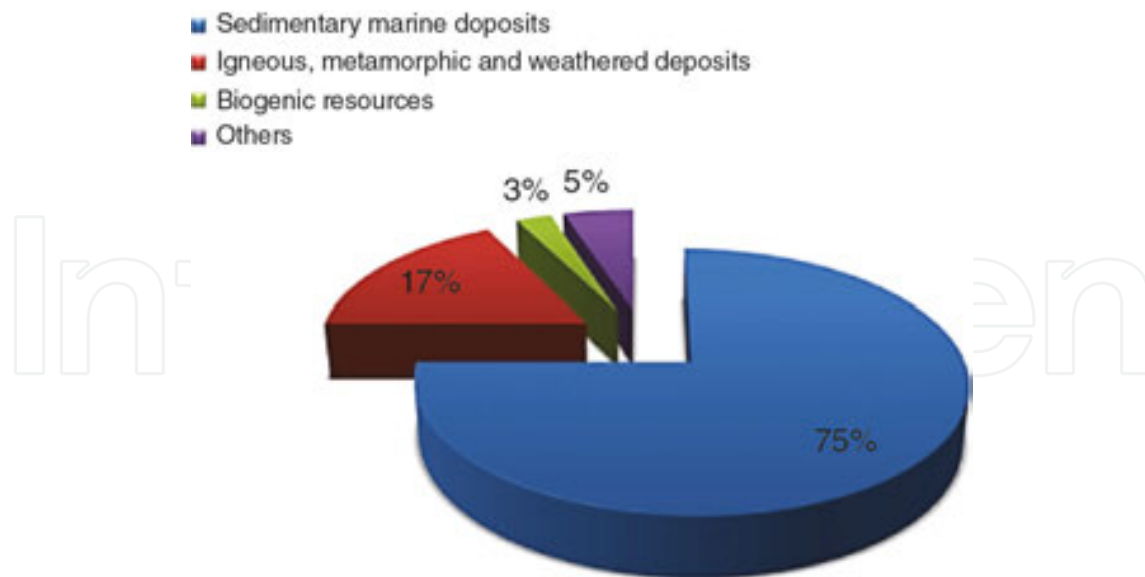
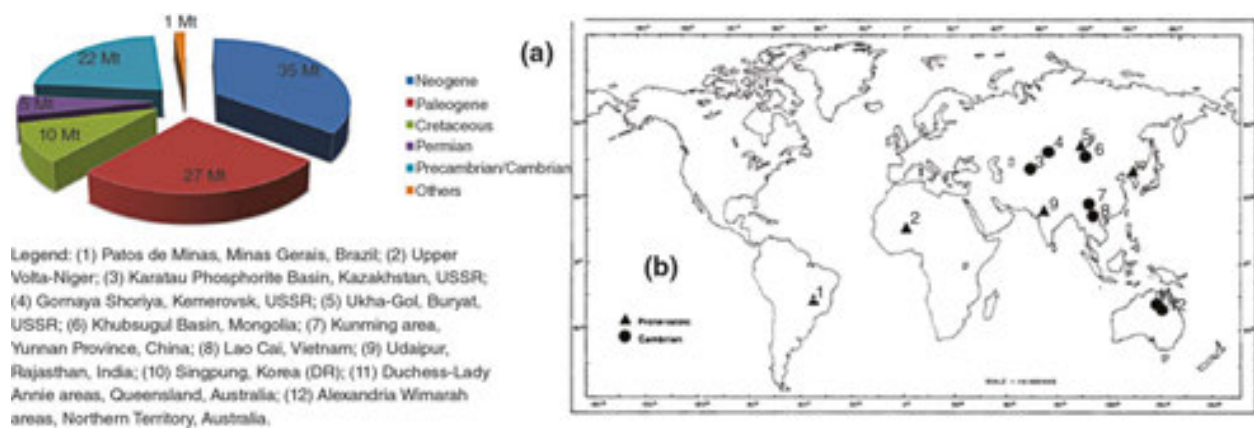


Fig. 2. The distribution of the world's phosphate resources [20].

<sup>4</sup> Most of the world's phosphate production comes from marine phosphorites [27].



**Fig. 3.** Stratigraphic distribution of phosphorites based on 1982 production data (a) and distribution of major Proterozoic-Cambrian phosphorites (b) [28].

The stratigraphic distribution<sup>5</sup> [29] of phosphorites [28] is shown in **Fig. 3(a)**. The major discoveries in Proterozoic and Cambrian rocks were not made until late 1930s, initially in the USSR (Kazakhstan), Poland, Korea, China and northern Vietnam. Early discoveries were made in the course of regional geological mapping and exploration for metal deposits, but later deposits were found mainly using more direct exploration techniques. It is possible that the greatest global phosphogenic episode in geological history took place in Late Proterozoic and Cambrian. While pelletal phosphorites are common in most Cambrian deposits, the Proterozoic age phosphorites contain mudstone (**Fig. 3(b)**, microphosphorite) and stromatolitic phosphorite<sup>6</sup> [28],[30].

Some phosphates were formed during all major sea-level transgressions during 67 million years of Cenozoic history; however, some periods were more important than others with respect to producing large volumes of phosphorites and preserving them in the geologic column. During the Paleocene and Eocene, several major episodes of phosphogenesis occurred within the major episodes of phosphogenesis in the major east-west ocean, which included Tethys [31],<sup>7</sup> producing extensive amounts of phosphorites throughout the Middle East, Mediterranean and northern South American regions. By the Neogene, this circum-global ocean had been destroyed by the plate tectonic processes, and the north-south Pacific and

<sup>5</sup> Since the Earth is stratified, in a broad sense, all rocks and classes of rocks (sedimentary, igneous and metamorphic) fall within the scope of stratigraphy and stratigraphic classification. Rocks can be classified according to lithology, fossil content, magnetic polarity, electrical properties, seismic response, chemical or mineralogical composition, etc. Rocks can be also classified according to time of their origin or environment of genesis. Rock bodies can be classified into many different categories of stratigraphic classification, including lithostratigraphic units (1), biostratigraphic units (2), chronostratigraphic units (3), unconformity-bounded units (4) and magnetostratigraphic units (5). Please see work [29] for further details.

<sup>6</sup> Phosphate occurs as concentrated in stromatolite columns, laminar algal (stromatolitic) phosphorite, reworked fragments of stromatolites forming silicified conglomeratic or brecciated phosphorite, massive-bedded phosphorite with sandy and clayey laminate and disseminate pellets and nodules in dolomite [30].

<sup>7</sup> The Tethys Ocean divided the continental masses into northern and southern groups. It merged at both ends with the Panthalassa or proto-Pacific Ocean. The remnants of Tethys are now located within Alpine mountain belts from the Caribbean in the west to recent collision zone between Australia and Eurasia in the east and within still-growing Central Atlantic Ocean between Africa and North America [31].

Atlantic oceans dominated global circulation patterns. Upper Cenozoic phosphogenesis (**Table 1**) occurred along the north-south ocean-ways, which now contain modern continental margins. On the basis of the extent of known phosphate deposits, the Miocene was by far the most important episode of phosphate formation in Upper Cenozoic [26].

Geological period		Age	Duration
Phanerozoic (541 <i>ma</i> to present)	Quaternary	Holocene	<3 <i>ma</i> 10 <i>ta</i>
	Cenozoic (66 <i>ma</i> to present)	258 <i>ma</i> to present	0.0117 <i>ma</i> to present
		Pleistocene	2.58 – 0.0117 <i>ma</i>
	Neogene	Pliocene	5 – 4 <i>ma</i> 1 <i>ma</i>
	23.03 – 2.58 <i>ma</i>	5.333 – 2.58 <i>ma</i>	
		Miocene	19 – 13 <i>ma</i> 6 <i>ma</i>
		23.03 – 5.333 <i>ma</i>	
		Paleogene	Oligocene 29 – 25 <i>ma</i> 4 <i>ma</i>
		66 – 23.03 <i>ma</i>	33.9 – 23.03 <i>ma</i>

*ma* – million years ago, *ta* – thousand years

**Table 1.** Formation of phosphorites during Upper Cenozoic phosphogenesis [26].

Phosphorites and phosphatic sediments are known on the floor of the Pacific, Indian and Atlantic oceans. They occur in a number of inshore areas (the shelves and upper part of the continental slopes) and in pelagic zones, chiefly on seamounts. Most of the shelf phosphorites are localized in four very large oceanic phosphorite provinces [32],[26],[33]:

- a. **East Atlantic:** Portugal, northwest Africa throughout South Africa and Agulhas Bank;
- b. **West Atlantic:** North Carolina throughout Florida, Cuba, Venezuela and Argentina;
- c. **East Pacific:** California throughout Baja California, Mexico and Peru throughout Chile;
- d. **West Pacific:** Sakalin Island, Sea of Japan, Indonesia, Chatham Rise east of New Zealand and East Australian shelf.

Sedimentary rocks with the content of 18 – 20 wt.% of  $P_2O_5$  are termed as phosphorites. The main phosphate mineral in phosphorites is carbonate-fluorapatite (CAF, francolite):  $Ca_{10-a-b-c}Na_aMg_b(PO_4)_{6-x}(CO_3)_{x-y-z}(CO_3,F)_y(SO_4)_zF_2$ , where  $x = y + a + 2c$  and  $c$  denotes the number of Ca vacancies, present as grain or mud. Most phosphorites are of marine origin [34],[35],[36]. Phosphorites on the sea floor occur in two types of environments on [37]:

- i. Continental margins in association with terrigenous;
- ii. Submerged mountains in association with calcareous and volcanogenic rocks.

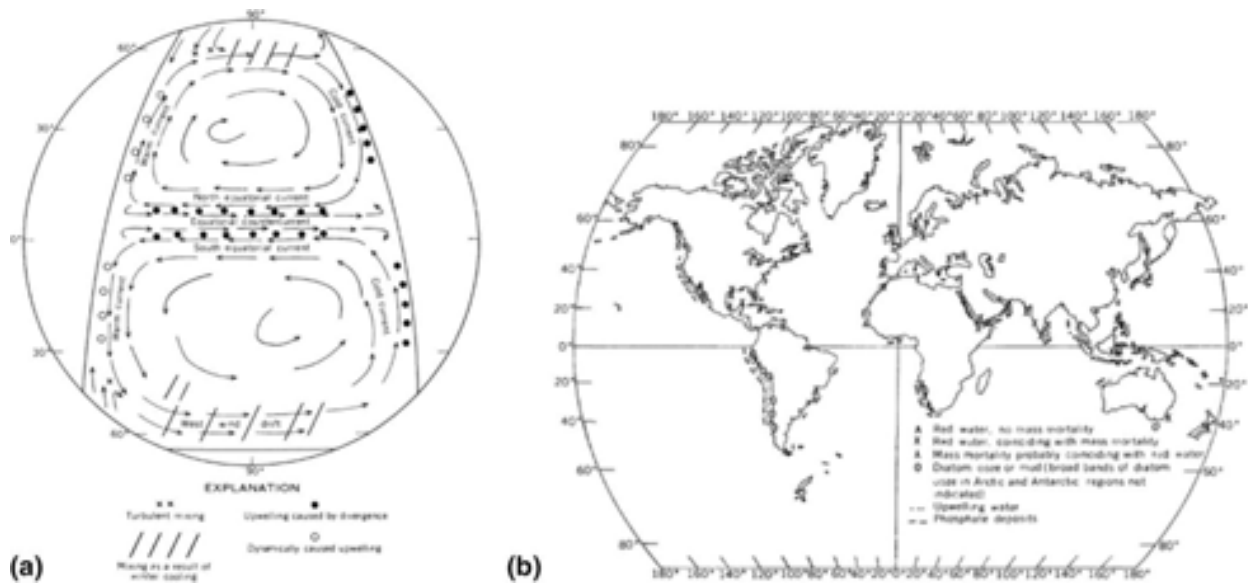


**Fig. 4.** The surface currents in an idealized ocean, showing the areas of ascending nutrient-rich water (a) and the distribution of upwelling water and related phenomena in modern oceans (b) [27].

Phosphorites consist mainly of phosphate cement enveloping small grains of phosphatic and non-phosphatic materials. Phosphate in the cavities of foraminifera is purer than that enveloping the grains [37].

The largest phosphorite-bearing regions are situated along the west coasts of Africa and America, at the east coast of the USA, off New Zealand and in the central part of the northern Pacific. The phosphatic matter of phosphorites consists of carbonate-fluorapatite and is intermixed with variable amounts of terrigenous, biogenic and diagenetic non-phosphatic components, which are the cause of a wide range of fluctuations in their chemical compositions. The age of sea-floor phosphorites varies from Cretaceous to Recent. Recent phosphorites are localized in the south west of Africa and at Peru-Chile shelves, which are the areas influenced by strong upwelling of nutrient-rich waters (**Fig. 4(a)**), resulting in high biological productivity, intensive biogenic sedimentation and diagenetic redistribution of geochemically active, mobile, organic-derived phosphorus in sediments. This phosphorus is accreted in the form of initially soft and friable nodules undergoing gradual lithification [27],[37].

Pronounced climatic, biological and geologic effects accompany upwelling, especially where it is produced by the divergence in coastal areas (**Fig. 4(b)**). The presence of cold waters along the coasts produces the coastal fogs and humid-air deserts, such as those of northern Chile and southwest Africa. The nutrient-rich waters that lie alongside these deserts are the lushest gardens of the sea, as the upwelling cold waters there support tremendous quantities of organisms. Most of large accumulations of guano (**Section 7.2.2**) are formed by the seafowl colonies feeding in these waters, and it is the extremely dry climate created by upwelling that makes the preservation of guano possible [27].

Sedimentary deposits usually contain varieties of carbonate-fluorapatite called francolite (described in **Section 2.6**). Francolite is defined as apatite that contains significant amount of

CO<sub>2</sub> with less than 1% of fluorine. Apatite associated with igneous source rocks may be of primary magmatic, hydrothermal or secondary origin. Primary apatite from igneous sources may be of fluorapatite, hydroxylapatite or chlorapatite varieties. Pure apatites from igneous deposits contain slightly over 42% of P<sub>2</sub>O<sub>5</sub> [23].

Since a wide range of very different particles and processes of formation complicates the simple classification of phosphorites, there is not any unified phosphorite classification<sup>8</sup> [18],[36],[38]. The proposed classification schemes for phosphorites describe their constituent particles, such as pelletal phosphorite. Nonetheless, the descriptor pelletal indicates nothing more than rounded phosphate particles of any origin. A widely recognized distinction in phosphorites is based on the grain size and holds specifically among phosphorites where the phosphate particles are of sand- or coarse silt-size and those that are of clay- and fine silt-size [28]. The phosphorites can be classified as follows [37]:

1. **Non-conglomeratic** (also termed as **nodular**) phosphorites: consist of phosphatized limestones and glauconite-quartz sandstones. Two varieties of nodular phosphorites can be recognized:
  - a. **Ferruginized** with glazed surface. The cement of ferruginized phosphorites is much richer in finely dispersed goethite than that of non-ferruginized phosphorites. Furthermore, ferruginized phosphorites do not contain the fragments of macrofauna.
  - b. **Non-ferruginized** with rough surface. In non-ferruginized phosphorites, the cement is micrite-collophane and its color varies from yellow (collophane, described in **Section 2.6**) to gray (micrite<sup>9</sup> [19]). The chambers of foraminifera are filled with phosphate-carbonate cement, less often with glauconite or goethite (FeO(OH) [33]).

Some nodules of phosphatized limestone are coated with a discontinuous layer of secondary phosphate with the thickness up to 1 cm.

2. **Conglomeratic phosphorites** consist of pebbles of phosphatized limestone (up to 50% of the rock) held together by the cement similar in composition to the phosphatized glauconite-quartz sandstones described above. In many samples of this type, two or three conglomerate layers are clearly visible, differing in size of pebbles and in content of glauconite. The bedding planes separating the layers with denser or less dense packing of grains are also distinguished in the cement. The surface of these planes is glazed and brown due to higher content of iron hydroxides and organic matter. Upon impact, the rock breaks along the planes. In addition, irregular microerosion surfaces are observed in

<sup>8</sup> The nature and origin of phosphorites have been a matter of much speculation since they were first discovered more than 150 years ago [38], and there is not any commonly accepted nomenclature [39].

<sup>9</sup> Micrite (the abbreviation for microcrystalline calcite) is characterized by crypto- to microcrystalline crystal texture. As the synonym of micrite, the names as lime mud, lime ooze, lime mudstone, calcimudstone and calcilitite are also used. The original definition sets a grain-size limit to < 4 μm, but current terminology distinguishes between minimicrite (<1 μm), micrite I (1 – 4 μm) and micrite II (4 – 30 μm). Furthermore, primary micrites (orthomicrites and nannoagorites), secondary micrites and pseudomicrites are recognized. Orthomicrites consist of subhedral polygonal calcite grains meeting at the interfaces. Nannoagorites are composed of calcareous pelagic biota. Secondary and pseudo micrites result from the diagenetic processes [19].

the conglomeratic phosphorites, which run across the grains of glauconite, shells and bedding planes [33].

The investigation of the microstructure of phosphorites by electron microscopy enables to recognize the following varieties [33]:

- i. **Gel-like**, phosphatized diatomaceous oozes, analogous (except phosphate content) to the enclosing diatomaceous oozes.
- ii. **Microgranular**, forming solid masses and globules from 1 to 3 mm in diameter. The rough surface of phosphate is caused by the fact that it consists of granules less than 0.1 mm in size.
- iii. **Fibrous**, constituting inner parts of globules.
- iv. **Ultramicrocrystalline phosphate**, forming a “jacket” on the surface of globules of amorphous phosphate. The size of crystal of apatite is 0.1 – 0.3  $\mu\text{m}$ .
- v. **Microcrystalline phosphate**, consisting of crystal of 1 – 3  $\mu\text{m}$  in size. Euhedral crystals are often formed in the cavities within the carbonate grains.
- vi. **Multiphase microgranular cement** consisting of carbonate, phosphate, quartz and layered silicates.

With regard to their texture and petrographic character, phosphorites can be classified according to the predominant size of the phosphorite component into four types [40]:

- a. **Microgranular (oolitic microgranular) phosphorites**, conditionally including aphanite: 0.01 – 0.1 mm;
- b. **Granular phosphorites**: 0.1 – 1 mm;
- c. **Nodular phosphorites**: 1 – 5 mm;
- d. **Shelly phosphorites**: 5 – 100 mm.

Although the types are named on the structural basis, the phosphate grains do not always have the dimensions given above. At the same time, the classified types fairly differ in many features, such as the association with various geological formations, the phosphate mineralogy and the stratigraphic sequence, thus being of lithologic character [40].

Most attempts to classify the phosphorite rocks adopt and modify the classification scheme for carbonates [36]. In 1962, DUNHAM [41] published the classification scheme for limestone. This scheme for carbonate rocks was modified for non-genetic classification of phosphorites (Fig. 5) [28].

Depositional texture recognizable					Depositional texture not recognizable
Original components not bound together during deposition				Original components were bound together during deposition as shown by intergrown skeletal matter, lamination contrary to gravity, or sediment-floored cavities that are roofed over by organic matter and are too large to be interstices	
Contains mud (particles of clay and fine silt size)		Grain-supported	Lacks mud and is grain supported		Boundstone
Mud-supported	Grain-supported				
Less than 10% grains	More than 10% grains				
Mudstone	Wackestone	Packstone	Grainstone	Boundstone	
Classification of phosphorites					
"Non-pelletal phosphorites"		"Pelletal phosphorites"			
Mudstone phosphorite	Wackestone phosphorite	Packstone phosphorite	Grainstone phosphorite	Boundstone phosphorite	

Fig. 5. The classification scheme of carbonate rocks modified for phosphorites [28].

The macroscopic classification scheme for phosphate sediments suggested by RIGGS [42] is shown in Fig. 6(a). The ancient deposits are better characterized via the scheme in Fig. 6(b), which was proposed by KASTERN and GARRISON [43]. In this model, three types of phosphates were recognized [39],[43]:

- i. F-phosphates are friable, light-colored micronodules and peloids of carbonate-fluorapatite (CFAP); they were formed by the precipitation of CFAP in laminated diatom muds deposited within the oxygen-minimum zone.
- ii. Phosphatic sands, termed as P-phosphates, consist of phosphatic peloids, coated grains and fish debris, often having an admixture of fine siliciclastic grains. These sands occur in thin layers and burrowed beds up to 2 m thick.
- iii. Dark and dense phosphates, herein called D-phosphates, are the most abundant. They occur as nodules, gravels and hard grounds. These phosphates were formed through complicated cycles of CFAP precipitation during early diagenesis, erosion and exhumation and reburial and rephosphatization processes associated with changing energy conditions, which may reflect the effects of changes in the sea level.

CFAP cements in P- and D-phosphates are often replaced microbial structures, but our data do not reveal whether this microbial involvement was passive or active. F-phosphates are most common in deeper water, outer-shelf/upper-slope sites, whereas D- and P-phosphates tend to predominate at shallower shelf sites more subjected to episodic high-energy conditions, especially during the low stands of sea level. This concept reveals the paleoenvironmental and time relationships of various phosphate sediments [39],[43].

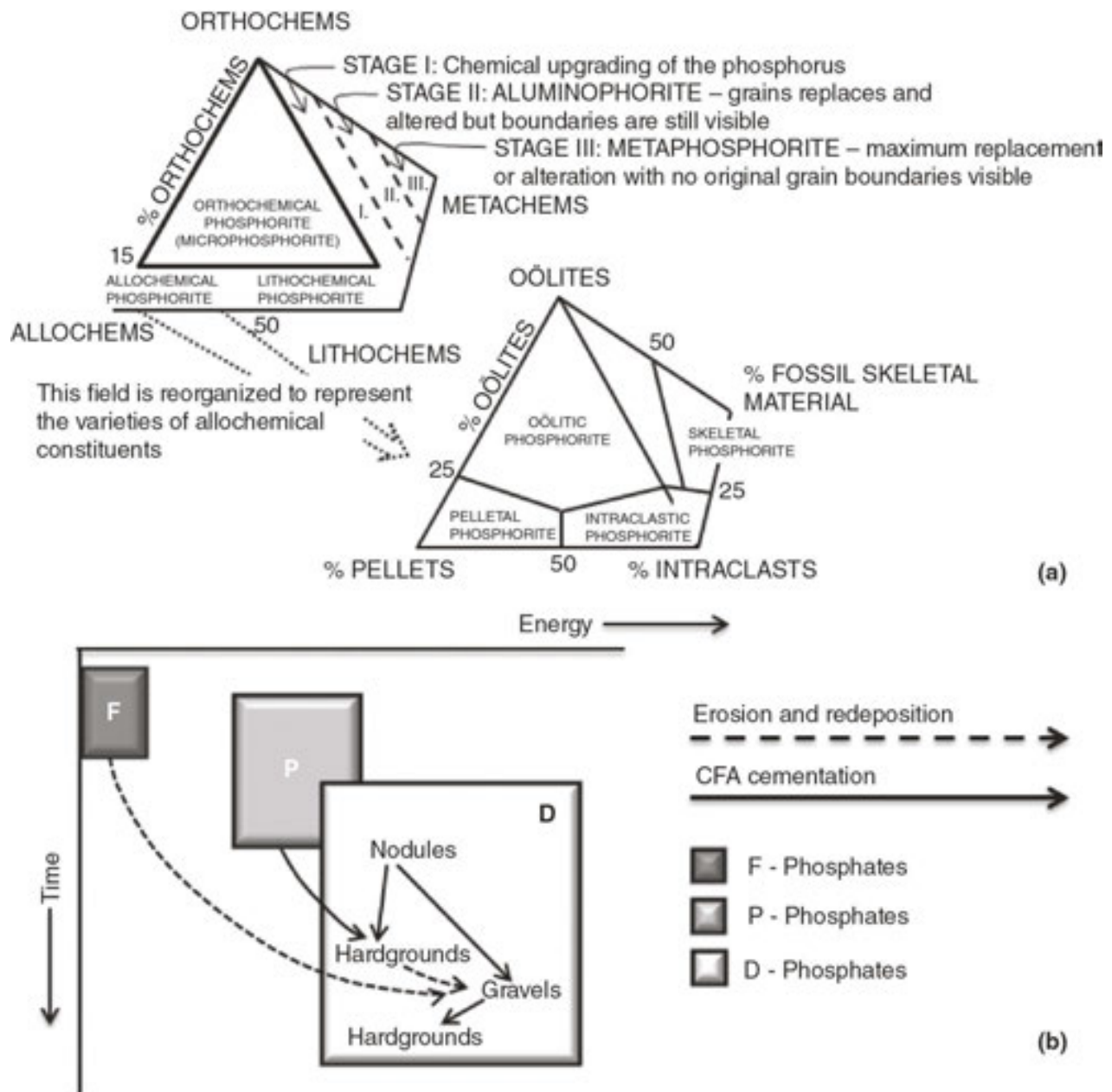


Fig. 6. The classification scheme of phosphorites proposed by RIGGS (a) and GARRISON and KASTNER [ 43 ].

Phosphorites can be formed in nature **authigenically** or **diagenetically**. In authigenesis, phosphorite forms as a result of the reaction of soluble phosphate with calcium ions forming corresponding insoluble phosphate compound. The role of microbes in these processes may be one or more of the following [44]:

- Making reactive phosphate available;
- Making reactive calcium available;
- Generating or maintaining the pH and redox conditions, which favor the precipitation of phosphate.

The models of authigenic phosphorite genesis (**Fig. 7**) assume the occurrence of mineralization of organic phosphorus in biologically productive waters, such as at ocean margins, that is, at shallow depths on continental slopes, shelf areas or plateaus [44].

Here, detrital accumulations may be mineralized at the sediment-water interface and in interstitial pore waters, liberating phosphate, some of which may then interact chemically with calcium in seawater to form phosphorite grains. These grains may be subsequently redistributed within the sediments units. The dissolution of fish debris (bones) is also considered an important source of phosphate in authigenic phosphorite genesis. The upwelling probably also plays an important role in many cases of authigenic formation of phosphorite. During non-upwelling period in winter, the phosphate-sequestering bacteria of oxidative genera *Pseudomonas* and *Acinetobacter* become dominant in the water column. Fermentative *Vibrios* and *Enterobacteriaceae* are dominant during upwelling in summer. It was suggested that *Pseudomonas* and *Acinetobacter*, which sequester phosphate as polyphosphate under aerobic conditions and hydrolyze polyphosphate under anaerobic conditions to obtain the energy of maintenance and to sequester volatile fatty acid from polyhydroxybutyrate formation,

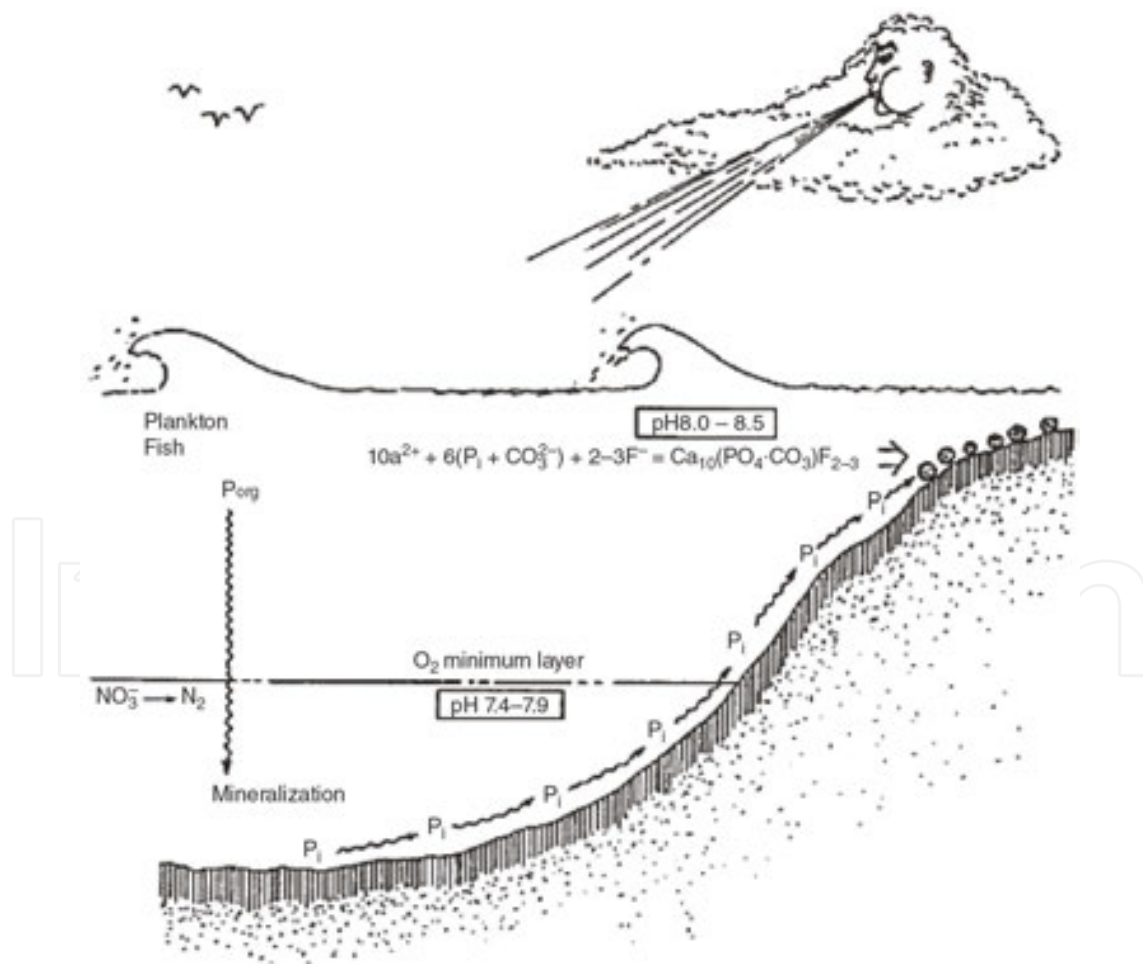


**Fig. 7.** The schematic presentation of formation of phosphorite in marine environment [44].

contribute to the phosphorite formation. Locally elevated, excreted orthophosphate becomes available for the precipitation as phosphorite by reacting with seawater calcium [44].

Authigenic phosphorite formation at some eastern continental margins, where upwelling, if occurred at all, was a weak and intermittent process that may have been formed more directly as a result of intracellular bacterial phosphate accumulation, which became transformed into carbonate-fluorapatite upon the death of cells accumulated in sediments in areas where the sedimentation rate was very low [44].

The model of diagenetic formation of phosphorite generally assumes the exchange of phosphate for carbonate in accretions that have the form of calcite and aragonite. The role of bacteria in this process is to mobilize phosphate by mineralizing detrital organic matter. The demonstration of this process in marine and freshwater environment under laboratory conditions leads to the hypothesis that the diagenesis of calcite to form apatite explains the origin of some deposits in the North Atlantic. The phosphorite deposits of Baja California and in the core of eastern Pacific Ocean seem to have formed as a result of partial diagenesis [44].

### 7.1.2. Igneous rocks

Apatites of igneous origin include hydrothermal veins and disseminated replacements, marginal differentiations near the boundaries of intrusions and pegmatites, but the largest deposits are intrusive masses or sheets associated with carbonatite, nepheline-syenite and other alkalic rocks [27]. Igneous rocks are classified on the basis of their [21],[45]:

1. **Color index:** means the volume percentage of dark-colored mineral and divides the rocks to **leucocratic** (color index varies from 0 to 30%), **mesocratic** (from 30 to 60%) and **melanocratic** (from 60 to 100%).
2. **Texture:** coarse-grained rocks, which crystallize at depth, are termed as **plutonic rocks** (as the rate of crystallization is slow, such rocks are holocrystalline<sup>10</sup>). Fine-grained rocks containing minerals embedded in glassy matrix<sup>11</sup> (often devitrified) are named as **volcanic** or **effusive rocks**. The crystallization of volcanic rocks takes place on the surface and is associated with rapid cooling and loss of volatile constituents of the lava. Their texture is therefore vesicular [46]<sup>12</sup> (vesicle-rich) and hypocrySTALLINE.<sup>13</sup>

Rocks that crystallize partly at depth and partly near the surface are called **hypabyssal**<sup>14</sup> (**subvolcanic**). The term **porphyry** is also related to hypabyssal rocks, which are characterized by one or more than one minerals present as phenocrysts in fine-grained ground-mass.

<sup>10</sup> The name for fully (100%) crystallized igneous rock [45].

<sup>11</sup> The matrix is defined as interstitial material between larger (skeletal) grains [46].

<sup>12</sup> The texture is characterized by many cavities (vesicles), which were formed by bubbles of volatile gasses during the decrease of pressure at extrusion of magma to the surface. Lava solidifies before bubbles of gases can escape to the atmosphere [46].

<sup>13</sup> The name for igneous rocks where the ratio of crystals to glassy phase is higher than 3:5. Rocks containing higher amount of glass are termed as hypohyaline or holohyaline [45].

<sup>14</sup> Denotes the intrusions of magma at shallow depths in the crust, often directly related to overlying volcanic edifices [45].

3. **Chemistry and mineralogy:** the rocks comprising more than 90 vol.% of ferromagnesian minerals, such as olivine, pyroxene, amphibole and biotite, are called **ultramafic (ultrabasic) rocks**. The rocks composed from essentially one or more ferromagnesian minerals are termed as **mafic**<sup>15</sup> (**basic**) **rocks**. In **mafelsic rocks**, the mafic and felsic minerals are present in approximately equal amounts. **Felsic rocks**<sup>16</sup> contain predominantly light-colored minerals, such as quartz, feldspar, feldspathoid and muscovite.

An acidic rock contains > 60% SiO<sub>2</sub>, whereas a basic rock is characterized by silica content ranging from 44 to 52% of SiO<sub>2</sub>. Many of ultramafic rocks are ultrabasic with the content of silica < 44%, but such ultramafic rocks as pyroxenites and amphibolites are not ultrabasic, but they are rather basic [21].

Igneous rocks are formed by the solidification of silicate melt from high temperatures. Since the sequence of crystallization follows the liquidus-solidus phase relationships, the minerals of low content will normally crystallize the least, but diorite and granodiorite melts may have enough phosphorus present for the FAP phase field to intersect the liquidus and to allow early formation of fluorapatite. Later-crystallizing phases should form in the interstices between early-crystallizing phases of alkali-rich igneous rocks and should form an immiscible phosphate-rich liquid phase, which leads to large late-stage segregations of FAP, some of which are associated with magnetite [47].

Where the content of phosphorus is very low, phosphorus may remain in the fluid phase, and apatite will form during the time at which the rock re-reacts with this fluid. This reaction is termed as pneumatolitic, and formed crystals will be small and often euhedral (with crystal facets). They may be included inside preexisting mineral grains. This situation is often encountered in granites and other related siliceous igneous rocks. The concentration of apatite minerals in igneous rocks is rarely sufficient to yield the source for mining the deposits for the phosphorus content [47].

### 7.1.3. Biogenic apatites

The biogenic (endogenous) mineral deposits form in surface environments as the transformation of primary organic aggregates or as a result of biochemical processes. Since the organism produces many of the same substances that form inorganically in rocks, the biogenic minerals are not minerals in the conventional sense<sup>1</sup>. Biogenic minerals originate from living organisms or with their assistance (**Table 2**). These compounds are crystallized within living organisms as a result of cell activity and are surrounded by organic matter. Classical examples are the bones of vertebrates. The bones and teeth consist of fine fibers or platy crystals (**Section 10.9.2**) of a mineral closely related to carbonate-hydroxylapatite (**Section 4.6**). These crystals are suspended in organic collagen. The crystals of apatite, which often do not exceed 10 nm in length, comprise up to 70% of weight of dried bone. The proteins make up the remaining 30% [48].

<sup>15</sup> Term mafic is the abbreviation of names of elements magnesium and iron (Latin word ferrum) [45].

<sup>16</sup> Term felsic is the abbreviator of names of minerals feldspar and silica [45].

Composition	Plant or animal examples
Silica (opal, chalcedony, quartz)	Radiolaria, siliceous sponges, diatomic algae
Carbonate Calcite	Archeocyatha, foraminifera, stromatoporoids, carbonate sponges, echinoderms, brachiopods, belemnites, ostracods, coccolithophora, cyanophycerae, purple algae, some mollusk shells, eggshells or birds and reptiles
Calcite crystals	Eyes of trilobites and brittle star
Aragonite	Corals, shells of mollusks and cephalopods
Aragonite transforming to calcite	Corals, bryozoa, gastropods, pelecypods
Phosphate Apatite	Bones, teeth, scales of vertebrates, brachiopods
Barite, gypsum	Ear stones of animals
Struvite	Kidney and gall stones
Oxalates Whewellite, weddellite	Kidney and gall stones
Phosphate-bearing carbonates	Brachiopods
Magnetite	In brain tissue of birds and insects (carrier pigeons, bees, etc.), bacteria ( <i>Magnetospirillum magnetotacticum</i> ). Magnetite is used for navigation and orientation.
Fe-hydroxides	Shells of diatoms, pediculates of Protozoa

**Table 2.** Mineralogical composition of solid plant and animal tissues [48].

In addition to the occurrence within the bones and teeth of vertebrates, mineral-organic aggregates are also found in mollusk shells, solid tissues of foraminifera corals, trilobites and other arthropods, echinoderms, some algae, etc. Some other biogenic processes involve bacteria. Large deposits of native sulfur, manganese oxides and hydroxides and iron are attributed to bacterial activity. Bacterial activity is also involved in the weathering processes of sulfide oxidation and transformation of kaolinite into bauxites [48].

Biogenic apatite is one of the most promising authigenic phases in this respect, as it is present in most siliciclastic deposits and is strongly enriched in a large suite of trace elements. Biogenic (fish teeth and bones) and diagenetic apatites are essential repositories of sedimentary phosphorus. They occasionally form huge deposits, as in West Africa, which are actively mined to provide agricultural fertilizers. Some of these deposits, found in particular in the Late Precambrian of China, after chemical precipitates seem to be associated with the episodes of global glaciation. In low-temperature waters, phosphates form numerous complexes. The concentration of phosphorus in sea and river water is limited by very low solubility of apatite. Phosphate radicals often attach to the surface of iron oxyhydroxide colloids when they precipitate in estuaries [49].

### 7.1.4. Genetic classification of phosphate rocks

The genetic classification proposed by EGOROV [50] includes three types of apatite ores according to the mineral assemblages [6],[51],[52],[53],[54],[55]:

- i. **Silicate-apatite (ijolite<sup>17</sup>):** ijolite is a medium- to coarse-grained equigranular rock composed of nephelite and aegirite-augite, or other pyroxene, in nearly equal proportions. There are varieties richer in nephelite, approaching the composition of urtite.<sup>18</sup> Nephelite is an equant anhedral, pyroxene forms euhedral crystals with zonal structure and margin of more sodic pyroxenes than that in the center, which is commonly titaniferous. Some varieties contain titaniferous melanite and iivaarite. Apatite is a prominent constituent and titanate is generally present in small amounts.
- ii. **Silicate-magnetite-apatite (phoscorite):** phoscorites<sup>19</sup> are spatially and temporally associated with carbonatites, often forming multiphase phoscorite-carbonatite series [56]. The term “phoscorite” was originally used to describe the magnetite-olivine-apatite rock with a carbonate core by RUSSELL et al [57],[58],[59].
- iii. **Carbonate-apatite (carbonatite):** the crystalline products of low-volume and high-temperature carbonate melts that have been evolving from the upper mantle (Fig. 8) for at least the past 2 Ga. Many are associated with crustal complexes of alkali-rich silicate rocks from which they may have evolved by liquid immiscibility.

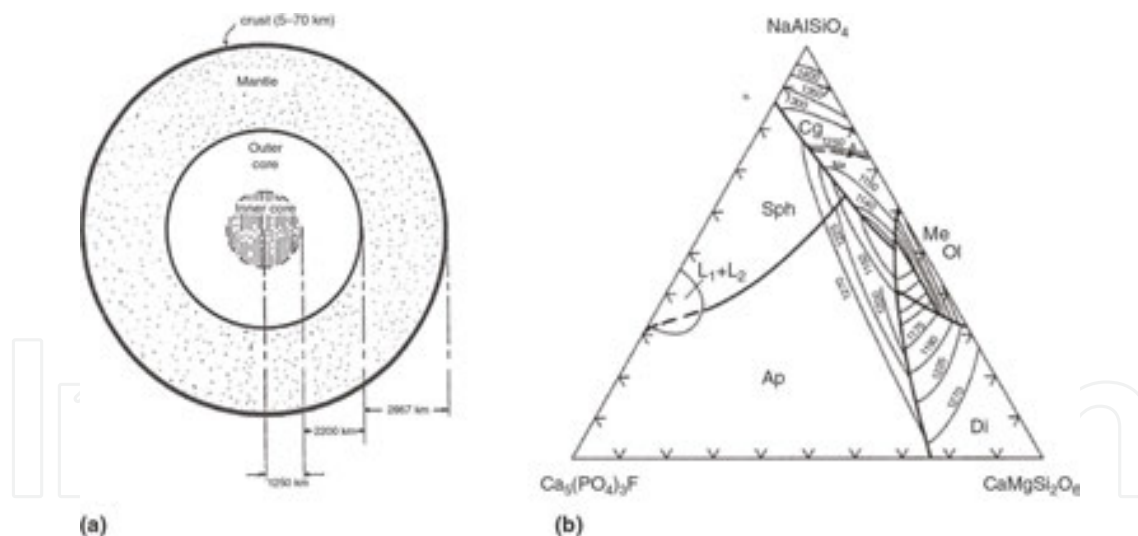


Fig. 8. The location of upper mantle on the cross-section of the Earth, core and mantle drawn to scale [44] (a). Ternary equilibrium phase diagram of the apatite bearing ijolite-urtite rock (b) approximated by the system  $\text{NaAlSiO}_4\text{-CaMgSi}_2\text{O}_6\text{-Ca}_5(\text{PO}_4)_3\text{F}$  [6]: olivine (Ol), melilite (Me), silicophosphate (Sph), apatite (Ap) and immiscibility field ( $L_1+L_2$ ).

<sup>17</sup> Ijolite, theralite and teschenite belong to phanerites (prelenic rocks characterized by equal or nearly equal amounts of femic components) [55].

<sup>18</sup> Urtite is medium-grained and light gray rock composed of about 70% nephelite, 25% aegirite or aegirite-augite [55].

<sup>19</sup> In the work [58], the name camaforite, i.e. Russian neologism [59], denotes the calcite-magnetite-forsterite assemblage, used as a synonym with phoscorite.

The endogenous apatite deposits can be classified<sup>20</sup> into the following types [60],[61]:

1. **Crystallized and concentrated in the late magmatic stage**, which can be further divided to (a) apatite-magnetite deposits (e.g. Kiruna deposit in Sweden) and (b) nepheline-apatite (e.g. Khibiny in Kola Peninsula in Russia).
2. **Skarns** (e.g. Ontario and Quebec in Canada).
3. **Carbonatites** (e.g. Sukulu in Uganda and Dorowa in Zimbabwe).
4. **Hypothermal veins with phlogopite** (e.g. Kaceres in Spain).
5. **Mesothermal type** (e.g. Toledo in Spain).
6. **Metamorphosed sedimentary phosphates** (e.g. Southern Peribaikalia, the Aldan massif in Russia (regional-metamorphosed subtype) and Karatau in Russia (contact-metamorphosis subtype)).
7. **Sedimentary phosphates**, which yield 85% of the world production, form in the sea by biochemical processes, in either:
  - **Geosynclinal sea**: e.g. in the Late Cretaceous and in Paleogene on the shelf of the Tethys geosyncline with the deposits in Morocco (Khouribga and Youssoufia), Algeria (Djebel Onk, El Kouit), Tunis (Gafsa), of the Permian geosyncline of the Rocky Mountains, with the deposits in the Phosphoria Formation in Idaho, Wyoming, Utah and Montana (USA), of the Caledonian geosyncline Karatau (Russia), large deposits are in the Upper Cretaceous in Kazakhstan, in the neighborhood of Aktyubinsk.
  - **Epicontinental sea**: e.g. in the Cenomanian of the south Russian digression and in the Jurassic of the Moscow region, at the margin of the African Shield in the Eocene complex near Hahotoe (Togo) and Taiba (Senegal), in the upper Cretaceous of Egypt [60].

## 7.2 Phosphate rock reserves

The Earth's crust contains about 0.27% of  $P_2O_5$ . About 200 minerals are known, which contain 1% or more  $P_2O_5$ . Movable concentrations of phosphate, containing from 5 to 35% of  $P_2O_5$ , are formed in all phases of the phosphate cycle (**Section 7.3.1**). The primary deposits include igneous apatites, sedimentary phosphorites and guano. The secondary deposits form from each of these as the result of weathering. Apatite is the principal primary mineral, but a number of others (**Section 7.5**) are common in the deposits formed during weathering of phosphate rocks and guano, e.g. brushite ( $CaHPO_4 \cdot 2H_2O$ ), monetite ( $CaHPO_4$ ), whitlockite ( $\beta-Ca_3(PO_4)_2$ ), crandallite ( $CaAl_3(PO_4)_2(OH)_5 \cdot H_2O$ ), wavellite ( $Al_3(OH)_3(PO_4)_2 \cdot 5H_2O$ ), taranakite ( $K_2Al_6(PO_4)_6(OH)_2 \cdot 18H_2O$ ), millisite ( $(Na,K)CaAl_6(PO_4)_4(OH)_9 \cdot 3H_2O$ ), variscite ( $AlPO_4 \cdot 2H_2O$ ) and strengite ( $FePO_4 \cdot 2H_2O$ ) [27].

<sup>20</sup> The classification according to DYBKOV and KARYAKIN.

### 7.2.1. Phosphate rock deposits

In general, phosphate rock reserves are non-metallic ores<sup>21</sup> that can be economically produced at the present time using existing technology. Phosphate rock resources include reserves and any other materials of interest that are not reserves. A reserve base is a portion of the resource from which future reserves may be developed. The classification applying to phosphate rocks include [23].

- **Resource** is defined as a concentration of naturally occurring phosphate material in such a form or amount for which the economic extraction of a product is currently or potentially feasible. The resources are divided into many categories depending on the amount of pertinent information available to define the amount of material potentially available and if it is economic, marginally economic or sub-economic to exploit these resources.
- **Reserve base** is the part of an identified resource that meets the minimum criteria related to current mining and production practices including grade, quality, thickness and depth.
- **Reserves** are the part of the reserve base that can be economically extracted or produced at the time of the determination. They may be termed as marginal, inferred or inferred marginal reserves. This does not signify that the extraction facilities are in place or functional.
- The grades of apatite deposits from the economic point of view are introduced in **Table 3**. The locations of the world's phosphate deposits are shown in **Fig. 9** and the average content of P<sub>2</sub>O<sub>5</sub> is listed in **Table 4**.

The most known Miocene phosphate deposits (**Table 1**) are in North Carolina, Florida, Venezuela, California, Baja California and Peru. In several cases, these emerged deposits are only the up dip limit of a larger Miocene section that extends seaward beyond the coastal plain and constitute large portions of the upper sediment regime that built the modern continental shelves [26].

Grade	P <sub>2</sub> O <sub>5</sub> [wt.%]	BLP [%]	Location
1 Economic	20	40.70	Florida and Moroccan sedimentary phosphorites, Kola and Palabora crystalline igneous apatites
2 Sub-economic	5 – 20	10.93 – 40.70	Western USA phosphoria, Russia nepheline-apatites
3 Non-economic	1 – 5	2.19 – 10.93	Low-grade ores, phosphatic limestones
4 Non-phosphatic	0.1 – 1.0	0.22 – 2.19	Widely distributed apatite in almost all igneous rocks

**Table 3.** Grades of apatite deposits [25].

<sup>21</sup> Ores of economic value can be classified as metallic or non-metallic according to the use of the mineral. Certain minerals may be mined and processed for more than one purpose. In one category, the mineral may be metal and non-metallic ore, e.g. bauxite used for the production of aluminum and ceramics, respectively [62].



Fig. 9. The overview of the world's phosphate deposits (a) [20] and the location of the major phosphate rock-producing areas of some known deposits (b) [26],[63].

Locally, these Miocene sediments are exposed on the seafloor; however, generally, they are buried below thin covers of Plio-Pleistocene and Holocene surface sediments. Thus, there is high potential for discovering new phosphate deposits within the Miocene sediments on the world's continental shelves, because [26]:

- a. Phosphate genesis is known to occur throughout the shelf in upper slope environments.
- b. Thicker and more extensive sequences of Miocene sediments occur on the shelves than on adjacent coastal plains.
- c. The shallow subsurface Neogene geology of most of the world's shelves is poorly known.

Source	% Source	%	Source	%
Fluorapatite	42 Tunisia (sedimentary)	28	Basic slag	10 – 20
Kola (igneous)	40 West USA (phosphoria)	18 – 30	Bone meal	20
Nauru (phosphorite)	39 Queensland	16 – 30	Guano	12 – 15
Florida (sedimentary)	35 Venezuela	20	California (seabed)	30
Kazakhstan	23 China (Yunnan)	32 – 36	Australia (Queensland)	24
Morocco (sedimentary)	35 Kola (nepheline)	12 – 20	—	—

**Table 4.** Grades of apatite deposits [25].

Two important sediment relationships were developed concerning reworked phosphate in surficial sediments on the North Carolina continental shelf [26],[63]:

- i. The distribution of phosphate in surface sediments closely reflects the distribution within underlying Miocene sediments units.
- ii. The process of reworking significantly dilutes the concentration of phosphate in the surficial sediments.

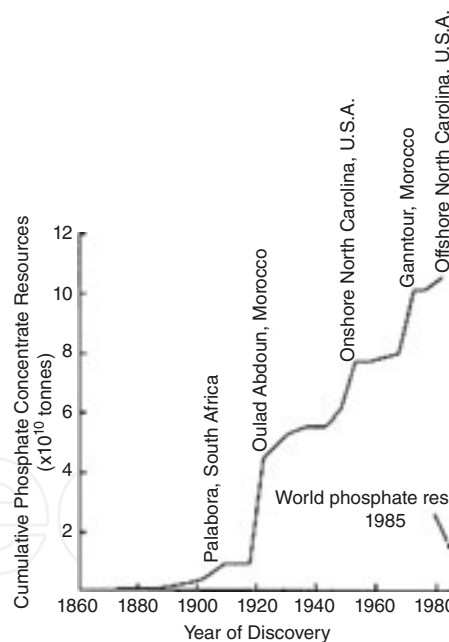


**Fig. 10.** The history of the discovery of the world's phosphate resources [22].

These relationships were also recognized on the shelves of northwest and southwest Africa and could represent important exploration tools for richer Tertiary<sup>22</sup> phosphorites occurring within the shallow subsurface on many continental shelves in the world [26].

<sup>22</sup> The term Tertiary (geologic period from 66 to 2.58 ma) is no longer recognized by the International Commission on Stratigraphy.

The deposits of apatite of igneous origin occur as intrusive masses or sheets, as hydrothermal veins or disseminated replacements, as marginal differentiations along or near the boundaries of intrusions or as pegmatites. Intrusive masses are the largest of these deposits. They are commonly associated with alkalic igneous rock complexes, many of which such as those in Africa, Brazil and Sweden are associated with the rift valley structures. Carbonatite, ijolite, nepheline-syenite and pyroxenite are common members of the rock assemblage. Many of these complexes have a ring like structure, with carbonatite as the central core [27].

Phosphate deposits have been discovered within the past 100 years at the rate far greater than the rate of consumption (Fig. 10). Since new phosphate deposits are expected to be discovered in the future, the oil exploration programs have probed most of the coastal sedimentary basins of the world during the past 20 – 30 years, and any large-scale discoveries of phosphate rock would probably have occurred in conjunction with these activities [22].

### 7.2.2. Other sources of phosphorus

Other important commercial sources of phosphorus (Table 4) include [25]:

- i. **Guano** [25],[27],[64],[65],[66]: natural deposit (accumulation) formed from decaying bones and excreta from fish-eating birds.<sup>23</sup> Fresh seafowl droppings contain about 22% N and 4% P<sub>2</sub>O<sub>5</sub>. Bat guanos are the most abundant in the cave areas of temperate and tropical regions. Although many bat guano deposits were found and mined, most of them are measured in hundreds or thousands of tons, and only sporadic production is obtained from them now. Seafowl deposits are mainly confined to islands and coastal regions at low latitudes. The largest lie along the west coasts of lower California, South America and Africa and on islands near the equatorial currents.

It was known that bird dung was utilized by the Carthaginians as early as 200 BC in order to improve crop yields. The content of P<sub>2</sub>O<sub>5</sub> in guano can vary in dependence on the age of the deposit,<sup>24</sup> the local climate and the bird kind. Guano deposits are found in Chile, Peru, Mexico, Seychelles, Philippines, the Arabian Gulf and elsewhere, but they account for less than 2% of the world's phosphate production.

Guano is used almost exclusively as fertilizers. The Nauru and Christmas Island phosphorite deposits may be guano in origin, but they are of very limited extent. It

---

<sup>23</sup> It is estimated that marine birds may take out as much as 5.10<sup>10</sup> g of phosphorus from the ocean each year [67]. The Spanish name "guano" has an origin in Quechua word "huanu" (i.e. dung).

Guano is composed of bird droppings, and although birds existed as early as the mid-Mesozoic, their major development did not occur until the Cenozoic era, probably in the Eocene period. It follows that some seamount deposits are too old to have originated from bird droppings [64].

Most of large accumulations of guano are formed on the surface by seafowl, but smaller quantities are formed by bats and to a lesser extent by other cave-dwelling mammals and birds [27].

<sup>24</sup> Recent guano contains 10 – 12% of P<sub>2</sub>O<sub>5</sub>, but leached guano contains 20 – 32%. The mineralogy of guano is complex. Slightly decomposed deposits contain soluble ammonium and alkali oxalates, sulfates and nitrates and a variety of magnesium and ammonium-magnesium phosphates. Deeply decomposed guano consists chiefly of calcium phosphates (for example, monetite or whitlockite) [27].

is believed that rainwater can carry soluble phosphate from guano and trickle over rocks, where phosphate interacts to form phosphatic layers, e.g. phosphatized coral rock. Bird guano, mainly from Peru, achieved the greatest importance in about the middle of the 19th century, shortly before the phosphate rock industry began to establish itself.

- ii. **Basic slag** [25]: is a minor source of phosphorus. This waste is the product from blast furnaces operating on iron ores with significant content of phosphorus. Basic slag contains tetracalcium phosphate ( $\text{Ca}_3(\text{PO}_4)_2 \cdot \text{CaO}$ ) and silicocarnotite ( $\text{Ca}_3(\text{PO}_4)_2 \cdot \text{Ca}_2\text{SiO}_4$ ), which are applied directly as fertilizers. Recorded world production is mainly from France, Germany and Luxembourg.
- iii. **Meat and bone meal (MBM) or bone ash** [25],[68]: as an animal byproduct, MBM contains not only substantial amounts of phosphorus in soluble organic form but also calcium and microelements. Ground (bone meal) or calcined and ground (bone ash) bones were recognized as a source of phosphorus at an early date.

Other important commercial sources of phosphorus are casein and lecithin. Casein is obtained from bovine milk. Lecithin was extracted from soy bean oil [25].

### 7.2.3. Phosphorite weathering derivatives

Weathering (**Section 7.3.2**) leads to the formation of enriched residual and replacing deposits from phosphatic deposits not otherwise minable. The Tennessee “brown rock” phosphate deposits consist of nowadays residuum developed through the decomposition of phosphatic limestones of Ordovician age. The “river pebble” deposits prominent in early history of phosphate mining in Florida and South Carolina are mostly placers formed by alluvial concentration of phosphatic pebbles eroded from the phosphatic formations of adjacent terrain [27].

The Tennessee “white rock” and Florida “hard rock” deposits were formed by the redeposition of phosphate derived from the decomposition of apatite under more advanced weathering. The same decomposition-phosphatization process accounts for the formation of calcium aluminum phosphate and aluminum phosphate in the “leached zone” of the Bone Valley field and deeply weathered Cretaceous and Eocene deposits of west Africa [27].

## 7.3. Geological role of apatite

As was described above, the number of different elements can substitute into the structure of apatite,<sup>25</sup> and this mineral can contain a number of trace elements by the substitution in both anion and cation sites. This means that apatite can be used as an indicator of planetary halogen compositions. The quantitative ion microprobe measurements of apatite from lunar basalts showed that portions of the lunar mantle and/or crust are richer in volatile species than previously thought [4].

<sup>25</sup> The tools based on the isotope composition of apatite were already described in **Section 6.5**.

Apatite was also used to determine the characteristics of metamorphic fluids within the mantle. For example, O'REILLY and GRIFFIN [69] and DOUCE et al [70] classified apatite within Phanerozoic mantle material into two geochemically distinct types:

1. **Apatite A:** is inferred to result from the metasomatism by CO<sub>2</sub>- and H<sub>2</sub>O-rich fluids derived from a primitive mantle source region;
2. **Apatite B:** compositions are consistent with the crystallization from magmas within the carbonate-silicate compositional spectrum.

This classification is based on halogen content, presence or absence of structural CO<sub>2</sub>, Sr and trace elements (especially U, Th and light rare-earth) and association with either metasomatized mantle wall-rock peridotites (Apatite A) or high-pressure magmatic crystallization products (Apatite B) [4],[69],[70].

In addition, apatite can be used as a probe to determine the petrogenetic evolution of granites, and significant amounts of research were devoted to the use of apatite in granitic rocks to distinguish between S- and I-type granites [4],[71].

The chemical composition of apatite is also a useful guideline for the petrogenetic and metallogenic history of magmas for the following reasons [4]:

- Apatite Eu and Ce anomalies provide the evidence of the redox state of the magmas that formed the host granitic rocks, with Eu enrichment and Ce depletion being indicative of oxidized magma and Eu depletion and Ce enrichment being indicative of reduced magma.
- Apatite <sup>87</sup>Sr/<sup>86</sup>Sr ratios reflect the Sr isotopic composition of the host granitic rocks.
- Apatite F and Cl concentrations can reflect the enrichment or depletion of halogens within the host granitoids, with apatite associated with slab dehydration containing more Cl and less F, whereas apatites related to magmas formed by partial melting of the crust contain less Cl and more F.

In recent sedimentary systems, the major phosphorus deposition occurs within upwelling zones at continental margins. Upwelling of deep ocean waters rich in phosphorus triggers high biological production in the photic zone and eventually high concentration of phosphorus in organic-rich sediments, as in recent Namibian and Peruan shelves [72],[73], [74],[75].

### 7.3.1. Cycle of phosphorus

In the Earth's crust, phosphorus takes the second place after carbon, and in comparison with all known elements, it takes about 12th place in natural abundance [25]. The phosphorus cycle is quite different from the nitrogen and sulfur cycles in which phosphorus is present in only one oxidation state and it forms no gases stable in biosphere or atmosphere. Also, in contrast to nitrogen and sulfur, substantial proportions of phosphorus in soil appear in inorganic form [76],[77].

About 10 Mt of phosphorus are released by weathering of apatite annually. In soil, monobasic (H<sub>2</sub>PO<sub>4</sub><sup>-</sup>) and dibasic (HPO<sub>4</sub><sup>2-</sup>) phosphates are generally available to plants. Phosphates

are precipitated by calcium in alkaline soils and most of phosphate is adsorbed on aluminum and iron oxides in acidic soils. Phosphates are most readily available in slightly acidic to neutral soil. Much of such phosphorus in surface soils appears in organic matter. This phosphorus is used repeatedly by recycling in plants and organisms that decompose the plant detritus. Little amount of phosphorus is lost by leaching through soils, but the erosion losses of soil particles and the plant detritus carried off to aquatic systems may be substantial [76].

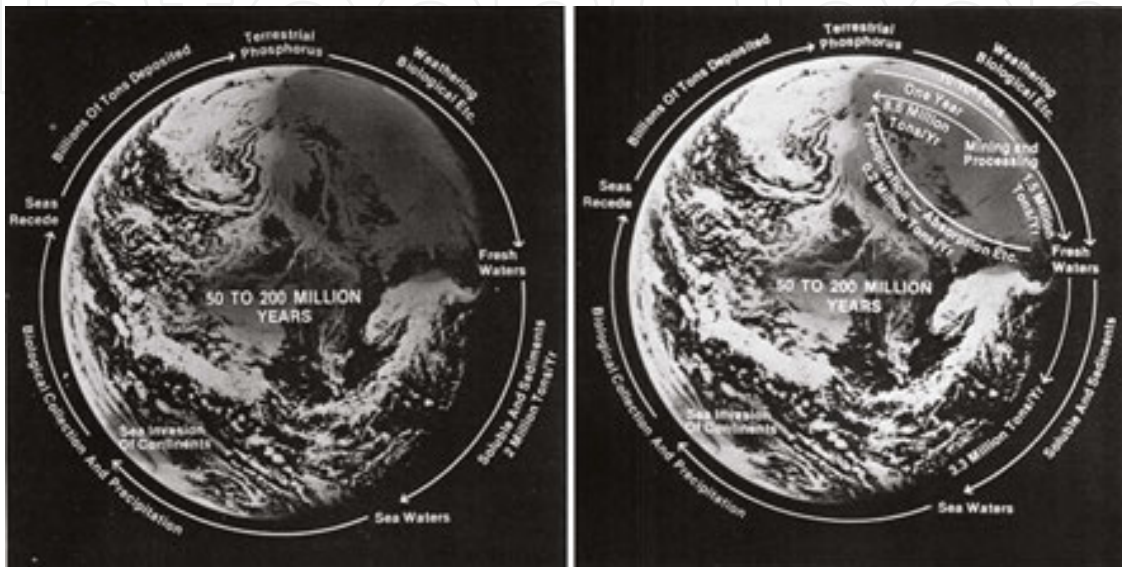


Fig. 11. Major natural cycle of phosphorus (a) and the contribution of the man to the cycle (b) [78].

The availability of phosphorus is a major factor limiting the biomass production in both terrestrial and aquatic ecosystems. Mycorrhizas are efficient scavengers of phosphorus for plants growing in soils with limited availability of this element. The phosphorus fertilization in agricultural lands can have detrimental effect, as it increases phosphate amounts in the runoff soil resulting in the accumulation of phosphate in aquatic plants and algal growth. If the decomposers of plants and algae use practically all oxygen from water, the habitat becomes unsuitable for fish and other aquatic animals. The process of abundant nutrient-induced biomass production in lakes and rivers and its decay to deplete the water oxygen is called the eutrophication [25],[76],[78].

Despite the advantage for which phosphorus is used, it is doubtful that man has significant contribution to the Earth's cycle of phosphorus (Fig. 11). The  $2 \cdot 10^9$  tons of mined phosphate rock is less than 0.15% of known reserves of phosphorus ore and less than  $1 \cdot 10^{-5}\%$  of the Earth's cycle of phosphorus [78].

At least 100 millions years before humankind exerted any influence on the cycles of phosphorus, the pattern had already been established (Fig. 12). Phosphorus was continuously leached from igneous rocks as the rocks were weathered to sedimentary deposits and this released phosphorus flowed to the seas, which had long since become saturated with phosphorus. Each new addition causes a similar quantity of phosphorus to precipitate as sediment. If the

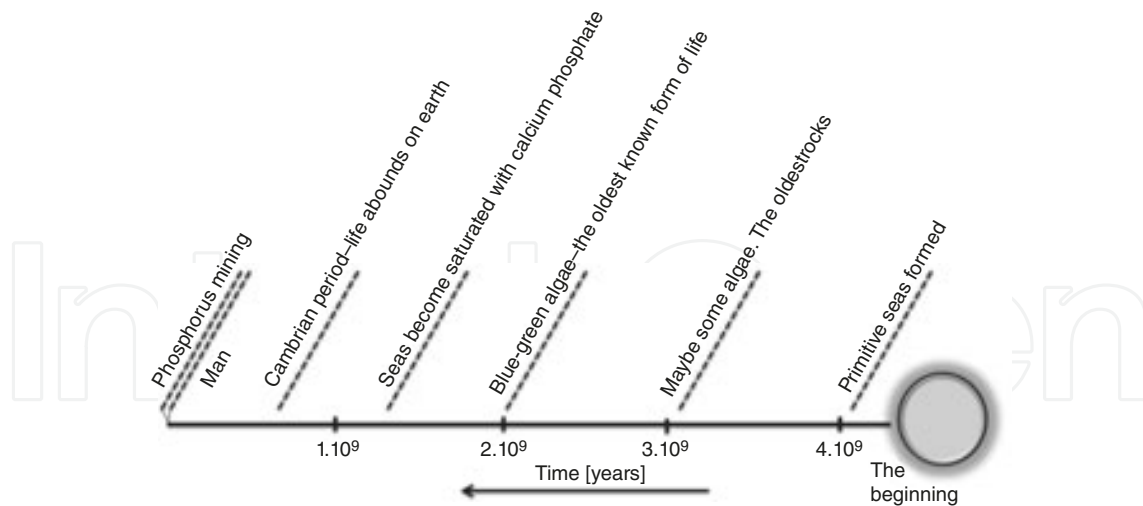


Fig. 12. The establishment of the Earth's cycle pattern of phosphorus [78].

precipitate formed when an island sea had invaded a land area, the new sediment became landlocked. The new landlocked sedimentary deposits are more easily leached than igneous rocks from which they are derived. When the seas recede sufficiently to expose the new sediments to the greater solvent action of fresh water, the sediments begin to weather and the cycle is complete. Best estimates of the cycle time of phosphorus in the oceans today are in the range of 50,000 years. This is a short period compared to  $3 \cdot 10^9$  years, which were required for the saturation of oceans for the first time [78].

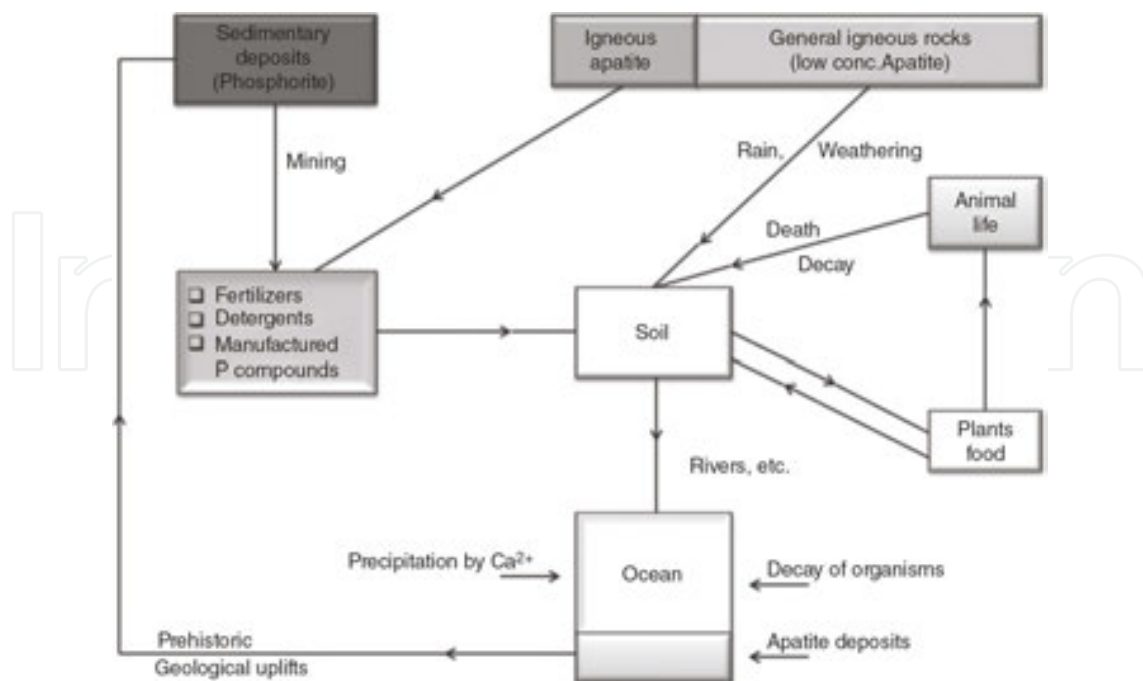


Fig. 13. Natural and artificial cycles of phosphorus [25].

Recently, man has only a slightly stronger influence on the total amount of the Earth's phosphorus than his prehistoric ancestors. If man made a significant alteration in the cycles of phosphorus, it had an impact on the cycles of fresh surface waters. The detergent phosphates have been blamed for degrading freshwater lakes and there is no doubt that several lakes have been overabundant with phosphates and sewage. Sewage treatment will alleviate most of the problems associated with point-source loading of lakes [78].

The overall natural and artificial cycles involving phosphorus are introduced in **Fig. 13**.

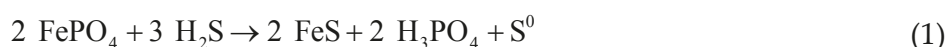
### 7.3.2. Weathering of apatite

Weathering and leaching processes from millions of years ago led to the transfer of phosphate to rivers and oceans where it was concentrated in shells, bones and marine organism that were deposited on the sea floor. Subsequent uplift and other geological movements led to these accumulations becoming dry land deposits [25],[78].

Generally, weathering of apatite occurs synergistically through biotic and abiotic processes and leads to the release of mineral phosphate. Inorganic phosphate cannot be assimilated by plants, but it can be converted to the bioavailable form orthophosphate ( $\text{HPO}_4^{2-}$ ,  $\text{H}_2\text{PO}_4^-$ ) by some species of phosphate-solubilizing fungi and bacteria. The main mechanism underlying the microbial phosphate solubilization is the secretion of organic acids that, by changing the soil pH and acting as chelators, may induce the dissolution of phosphorus from minerals and its release into the pore water of soils [79],[80]. The dissolution of apatite is described in **Section 3.4**.

Apatite represents an important source of inorganic P for natural ecosystems and may favor the establishment of microbial communities able to exploit it [79]. The microorganisms can cause the fixation or immobilization of phosphate, either by promoting the formation of inorganic precipitates or by the assimilation of phosphate into organic cell constituents on intracellular polyphosphate granules. Insoluble forms of inorganic phosphorus, e.g. calcium, aluminum and iron phosphates, may be solubilized through the microbial action. The mechanisms by which the microbes accomplish this solubilization vary [44]:

- i. The first mechanism may be the production of inorganic or organic acids that attack the insoluble phosphates.
- ii. The second mechanism may be the production of chelators such as gluconate and 2-ketogluconate, citrate, oxalate and lactate. All these chelators can complex the cation portion of insoluble phosphate salts and thus force their dissociation.
- iii. The third mechanism of phosphate solubilization may be the reduction of iron in ferric phosphate, e.g. strengite ( $\text{Fe}^{3+}\text{PO}_4 \cdot 2\text{H}_2\text{O}$  [81]), to ferrous iron by enzymes and metabolic products of nitrate reducers such as *Pseudomonas fluorescens* and *Alcaligenes* spp. in sediments.
- iv. The fourth mechanism is the production of hydrogen sulfide ( $\text{H}_2\text{S}$ ), which can react with iron phosphate and precipitate it as iron sulfide, thereby mobilizing phosphate, as in the reaction [44]:



The phosphate-solubilizing ability is a feature of many free-living and plant-symbiotic bacterial taxa, such as [79]:

- *Pseudomonas* [82]: the genus *Pseudomonas* sensu stricto comprises many species characterized by their metabolic diversity and by a wide range of niches that they can colonize.
- *Rhizobium* [83]: specific group of bacteria that have the capability of symbiotic nitrogen fixation.
- *Burkholderia* [84]: aerobic, non-spore-forming bacteria. *Burkholderia* is very versatile and occupies a wide range of ecological niches.

Microbial rock weathering is common in all climate zones and usually acts very slowly [80].

### 7.3.3. Fission track and apatite fission-track analysis

The fission-track (FT) dating is a radiometric dating method<sup>26</sup> based on the analysis of radiation damage trails (fission tracks) in uranium-bearing, non-conductive minerals and glasses. It is routinely applied to the minerals apatite, zircon and titanite. Fission tracks are produced continuously through geological time as a result of spontaneous fission track of <sup>238</sup>U atoms<sup>27</sup> that undergo spontaneous fission.<sup>28</sup> The atom splits into two parts that move rapidly in opposite directions, creating a long thin region of damage. The submicroscopic features with an initial width of approximately 10 nm and the length of up to 20 μm can be revealed by chemical etching.<sup>29</sup> Crucially, fission tracks are semi-stable features that can self-repair (shorten and eventually disappear) by the process known as annealing at a rate that is a function of both time and temperature. The extent of any track shortening (exposure to elevated temperatures) in a sample can be quantified by examining the distribution of fission-track lengths [6], [85],[86],[87],[88].

This unique sensitivity of the apatite fission-track system is now of considerable economic importance due to the coincidence between the temperature range over which annealing occurs and that over which liquid hydrocarbons are generated. Other applications include the determination of timing of emplacement and the thermal history of ore deposits. There is

<sup>26</sup> Radiometric dating techniques are, in general, complementary to one another, and each method produces an age with the special meaning, such as the last outgassing, the last melting accompanied by mixing with isotopically separate material and the last heating to remove the track. Fission-track dating is conceptually the simplest of several dating techniques that provide absolute measures of time from slow but statistically steady decay of radioactive nuclides [86].

<sup>27</sup> Most radiometric dating processes are based on the statistical regularity of the decay of one parent radionuclide into a daughter nuclide, for example, <sup>40</sup>K into <sup>40</sup>Ar, <sup>87</sup>Rb into <sup>87</sup>Sr or <sup>238</sup>U, <sup>235</sup>U and <sup>232</sup>Th into <sup>206</sup>Pb, <sup>207</sup>Pb and <sup>208</sup>Pb, respectively. The age of sample can be then determined by measuring relative abundance of parent and daughter in any pair. The major isotope of uranium (<sup>238</sup>U) decays at a spontaneous rate of ~10<sup>-16</sup> per year [86].

<sup>28</sup> Fission track can also be created artificially (induced track) by irradiating the mineral specimen with thermal neutrons in a nuclear [88].

<sup>29</sup> The mineral grain is ground and polished to expose a flat surface inside the crystal. It is then immersed in a chemical etchant that preferentially attacks the regions of damage, widening them and making them visible under optical microscope. The track appears in the apatite torch readily in 20 to 30 s when immersed in diluted nitric acid [88].

abundant literature on both fission-track dating and its use in evaluating the tectonic and thermal history of rocks [6],[89],[90],[91].

Apatite is the most frequently used material for fission-track dating [92]. Apatite fission-track (AFT) analysis serves as a thermochronological tool to investigate the low-temperature thermal history of rocks below  $\sim 120^\circ\text{C}$  [93],[94]. The estimates of closure temperatures for fission-track retention in apatite are usually in the range from 75 to  $120^\circ\text{C}$  at cooling rates between 1 and  $100^\circ\text{C}/\text{m.y.}$  [6].

Thermochronology may be described as the quantitative study of the thermal histories of rocks using temperature-sensitive radiometric dating methods such as  $^{40}\text{Ar}/^{39}\text{Ar}$  and K-Ar, fission track and (U-Th)/He. Among these different methods, apatite fission track and apatite (U-Th-Sm)/He (AHe) are now, perhaps, the most widely used thermochronometers, as they are the most sensitive to low temperatures (typically between  $40$  and  $125^\circ\text{C}$  for the durations of heating and cooling in the extent of  $10^6$  years). They are ideal for investigating the tectonic and climate-driven surficial interactions that take place within the top few ( $<5$  km) kilometers of the Earth's crust. These processes govern the landscape evolution, influence the climate and generate the natural resources essential to the well-being of mankind [85],[95].

#### 7.3.4. Extraterrestrial apatite

On Earth, magmatic volatiles (i.e.  $\text{H}_2\text{O}$ , F, Cl, C-species and S-species) play an important role in the physicochemical processes that control thermal stabilities of minerals and melts, in magma eruptive processes and in the transportation of economically important metals. On the Moon, magmatic volatiles in igneous systems are poorly understood, and the magmatic volatile inventory of lunar interior, aside from being very low, is not well constrained. Although the Moon is a volatile-depleted planetary body, there is evidence indicating that magmatic volatiles have played a role in igneous processes on the Moon. Specifically, magmatic volatiles were implicated as the propellants that drove fire-fountain eruptions, which produced the pyroclastic glass deposits encountered at the Apollo 15 and 17 sites [96]. That is supported by recent discoveries of water-rich apatite from lunar mare basalts [97],[98].

Apatite was found in a large number of samples of igneous lunar rocks, although it typically occurred in only trace amounts and is typically reported as coexisting with REE-merrillite  $[(\text{Mg,Fe})_2\text{REE}_2\text{Ca}_{16}\text{P}_{14}\text{O}_{56}]$ , and those two minerals make up the primary mineralogical budget for P on the Moon [96]. Merrillite, also known as the mineral whitlockite (or more precisely and dehydrogenated whitlockite) [99], is one of the main phosphate minerals, along with apatite, which occur in lunar rocks, in Martian meteorites and in many other groups of meteorites. Significant structural differences between terrestrial whitlockite and lunar (and meteoritic) varieties require the use of "merrillite" name for the H-free extraterrestrial material, and the systematic enrichment of REE in lunar merrillite requires the use of "REE-merrillite". Lunar merrillite, ideally  $(\text{Mg,Fe}^{2+},\text{Mn}^{2+})_2[\text{Ca}_{18-x}(\text{Y,REE})_x](\text{Na}_{2-x})(\text{P,Si})_{14}\text{O}_{56}$ , contains high concentrations of Y + REE [100],[101].

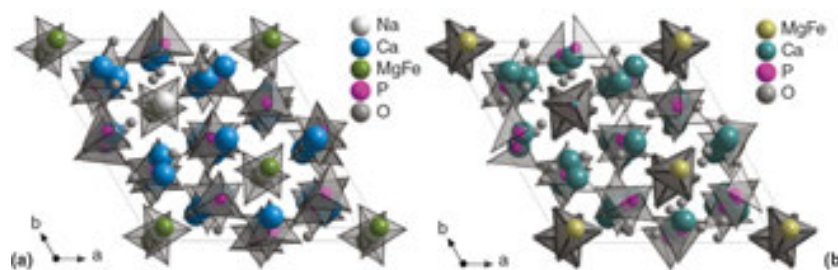


**Fig. 14.** The structure of lunar merrillite (a) [102] and terrestrial whitlockite (b).

Lunar merrillite (**Fig. 14(a)**), trigonal, the space group R3c with the cell parameters  $a = 10.2909 \text{ \AA}$ ,  $c = 36.8746 \text{ \AA}$ ,  $c:a = 3.5832$  and  $V = 3381.93 \text{ \AA}^3$ ) and terrestrial whitlockite (**Fig. 14(b)**), trigonal, the space group R3c with the cell parameters  $a = 10.3300 \text{ \AA}$ ,  $c = 37.1030 \text{ \AA}$ ,  $c:a = 3.5918$  and  $V = 3428.79 \text{ \AA}^3$ ) have largely similar atomic arrangements, but the phases differ due to the presence or absence of hydrogen. In whitlockite, H is an essential element and allows the charge balance. Hydrogen is incorporated into the whitlockite atomic arrangement by disordering one of the phosphate tetrahedra and forming the  $\text{PO}_3(\text{OH})$  group. Lunar merrillite is devoid of hydrogen; thus, no disordered tetrahedral groups exist. The charge balance for the substituents Y and REE (for Ca) is maintained by  $\text{Si}^{4+} \leftrightarrow \text{P}^{5+}$  tetrahedral substitution and  $\square \leftrightarrow \text{Na}^+$  substitution at Na site [99],[102].

A number of sources potentially contributed to the overall inventory of lunar water, including primary indigenous water acquired during lunar accretion, late addition of water through asteroidal and cometary impacts and solar wind implanting H into lunar soils. The average D/H ratios of apatite in norite (Apollo sample 78235) and in the granite clast (14303) are consistent with the estimates for the H isotopic composition of recent bulk-Earth and terrestrial mantle. By contrast, the average H isotopic composition of apatites in norite 77215 is lower. The content of water in norite parental melts provides strong evidence that the magmas involved in secondary crust production on the Moon were hydrated, in agreement with recent findings of water in lunar ferroan anorthosites. Water they contain, locked in the crystalline structure of apatite, is characterized by an H isotopic composition similar to that on Earth and in some carbonaceous chondrites [103].

Apatite preserves a record of halogen and water fugacities that existed during the waning stages of crystallization of planetary magmas, when they became saturated in phosphates. The thermodynamic formalism based on apatite-merrillite equilibria that makes it possible to compare the relative values of halogen and water fugacities in Martian, lunar and terrestrial basalts, accounting for possible differences in pressure, temperature and oxygen fugacities among the planets, was described by DOUCE and RODEN [104].

They showed that planetary bodies have distinctive ratios among volatile fugacities at apatite saturation and that these fugacities are, in some cases, related in a consistent way to volatile fugacities in the mantle magma sources. Their analysis shows that the Martian mantle parental to basaltic SNC meteorites was dry and poor in both fluorine and chlorine compared to the terrestrial mantle. Limited data available from Mars show no secular variations in mantle halogen and water fugacities from  $\sim 4 \text{ Ga}$  to  $\sim 180 \text{ Ma}$ . Water and halogens found in recent

Martian surface rocks have thus resided in the planet's surficial systems since at least 4 Ga and may have been degassed from the planet's interior during the primordial crust-forming event. In comparison to the Earth and Mars, the Moon, and possibly the eucrite parent body too, appear to be strongly depleted not only in H<sub>2</sub>O but also in Cl<sub>2</sub> relative to H<sub>2</sub>O. The chlorine depletion is the strongest in mare basalts, perhaps reflecting an eruptive process characteristic with large-scale lunar magmatism [104].

Mars does not recycle crustal materials via the plate tectonics. For this reason, the magmatic water reservoir of the Martian mantle has not been affected by the surface processes, and the deuterium/hydrogen (D/H) ratio of this water should represent the original primordial Martian value. Following this logic, hydrous primary igneous minerals on the Martian surface should also carry this primordial D/H ratio, assuming no assimilation of Martian atmospheric water during the crystallization and no major hydrogen fractionation during the melt degassing. Hydrous primary igneous minerals, such as apatite and amphibole, are present in Martian meteorites here on Earth. Provided these minerals have not been affected by terrestrial weathering, Martian atmospheric water or shock processes after the crystallization, they should contain a good approximation of the primordial Martian D/H ratio. As Nakhla was seen to fall on the Egyptian desert in 1911, the terrestrial contamination is minimized in this meteorite. The nakhlites are also among the least shocked Martian meteorites. Therefore, apatite within Nakhla could contain primordial Martian hydrogen isotope ratios. The similar D/H ratios indicate that the Earth and Mars, and possibly the other terrestrial planets, accreted water from the same source [105].

Vesta, as the second most massive asteroid, has long been perceived as anhydrous. Recent studies suggesting the presence of hydrated minerals and past subsurface water have challenged this long-standing perception. The volatile components indicate the presence of apatite in eucrites. Eucritic apatite is fluorine rich with minor chlorine and hydroxyl (calculated by difference) [106],[107],[108].

#### 7.4. The future of phosphate rocks

The biochemist and sci-fi author IZAAK ASIMOV said [60]: "In the future coal will be probably substituted by nuclear energy, wood by plastics, meat by yeast and suspecting solitude by friendship, but there is no substitute for phosphorus."

The search for phosphate rock deposits became a global effort in the 20th century as the demand for phosphate rocks increased. The development of deposits further intensified in the 1950s and 1960s. The world production reached its peak in 1987 – 1988 and then again in 2008 with over 160 million metric tons (mmt) of the product. Phosphate rock mining has evolved over time, and worldwide, it relies on high volume and advanced technology using mainly open-pit mining methods and advanced transportation systems to move hundreds of millions of tons of overburden to produce hundreds of millions of tons of ore, which are beneficiated to produce approximately 160 mmt of phosphate rock concentrate per year. The concentrate of suitable grade and chemical quality is then used to produce phosphoric acid,

the basis of many fertilizer and non-fertilizer products [23]. The world phosphate production rate since 1850 according to JASINSKI [109] and ABOUZEID et al [20] is shown in Fig. 15.

The estimates of the world's phosphate reserves and availability of exploitable deposits vary greatly and the assessments of how long it will take until these reserves are exhausted vary also considerably. Furthermore, it is commonly recognized that the high-quality reserves are being depleted expeditiously and that the prevailing management of phosphate, a finite non-renewable source, is not fully in accordance with the principles of sustainability. The depletion of current economically exploitable reserves is estimated to be completed in some 60 to 130 years. Using the median reserve estimates and under reasonable predictions, it appears that phosphate reserves would last for at least 100+ years [20].

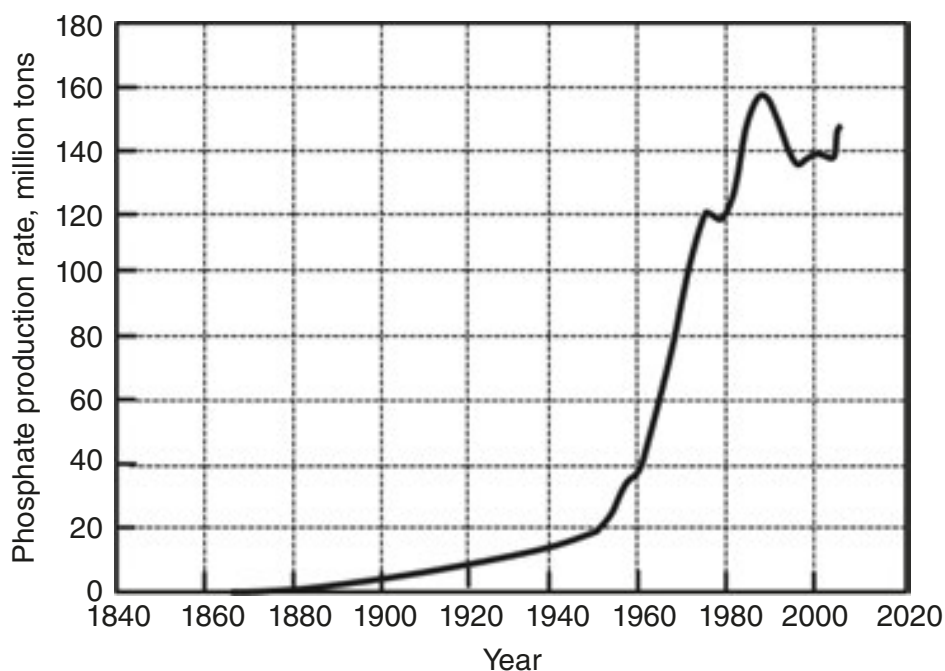


Fig. 15. World phosphate production rate [20].

Preliminary estimates of phosphate rock reserves range from 15,000 mmt to over 1,000,000 mmt, while the estimates of phosphate rock resources range from about 91,000 mmt to over 1,000,000 mmt. Using available literature, the reserves of various countries were assessed in the terms of reserves of concentrate. The IFDC<sup>30</sup> estimate of worldwide reserve is approximately 60,000 mmt of concentrate. Based on the data gathered, collated and analyzed for the IFDC report, there is no indication that a “peak phosphorus” event will occur in 20 – 25 years. Based on the data reviewed, and assuming current rates of production, phosphate rock concentrate reserves to produce fertilizers will be available for the next 300 – 400 years [23].

Phosphate rock prices will increase when the demand approaches the limits of supply. When the phosphate rock prices increase, some resources will become reserves, marginal mining

<sup>30</sup> International Fertilizer Development Center.

projects will become viable and the production will be stimulated. In the future, fuel and fuel-related transportation costs may become even more important components in the world phosphate rock production scenario. The political disruption is always an unknown factor, and it can profoundly influence the supply and demand for fertilizer raw materials on a worldwide basis [22].

## 7.5. Non-apatitic phosphate minerals

Apart from those in the supergroup of apatite minerals, the well-known phosphate minerals include [25]:

1. **Autunite** [110],[111]: is orthorhombic mineral (space group  $I4/mmm$ ) of the composition of  $(Ca[(UO_2)(PO_4)]_2(H_2O)_{11})$ , **Fig. 16**, which crystallizes in the space group  $Pnma$  with the cell parameters:  $a = 14.0135 \text{ \AA}$ ,  $b = 20.7121 \text{ \AA}$ ,  $c = 6.9959 \text{ \AA}$ ,  $V = 2030.55 \text{ \AA}^3$  and  $Z = 4$ . It belongs to the most abundant and widely distributed uranyl phosphate minerals. The structure contains the well-known autunite-type sheet with the composition  $[(UO_2)(PO_4)]^-$  resulting from the sharing of equatorial vertices of uranyl square bipyramids with phosphate tetrahedra. Calcium atom in the interlayer is coordinated by seven  $H_2O$  groups and two longer distances to uranyl apical O atoms. Two symmetrically independent  $H_2O$  groups are held in the structure only by hydrogen bonding. The bond-length-constrained refinement provides a crystal-chemically reasonable description of the hydrogen bonding.

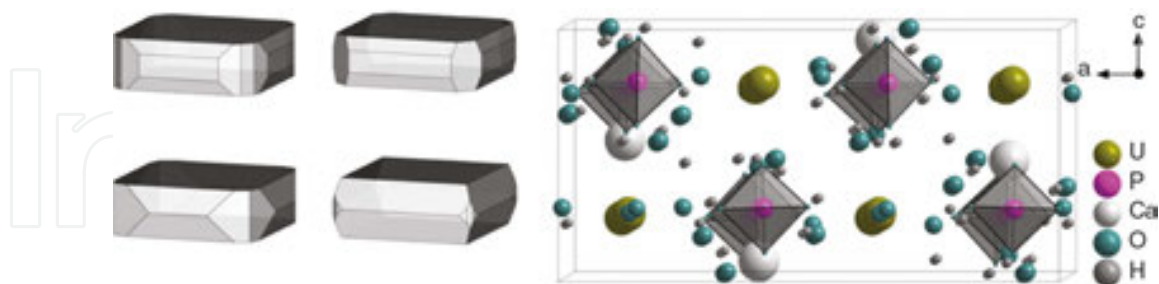


**Fig. 16.** The examples of forms and the structure of mineral autunite [110] viewed along the b-axis.

The mineral was named by HENRY J. BROOKE and WILLIAM H. MILLER in 1854 after the typical locality at Saint Symphorien, Autun District, Saône-et-Loire, France. Autunite dehydrates rapidly in air (except for high relative humidity) to tetragonal meta-autunite ( $P4/nmm$ ,  $a = 6.96 \text{ \AA}$ ,  $c = 8.40 \text{ \AA}$  and  $c:a = 1.21$ ) [112]. The loss of O12 and O13 from autunite results in the formula  $Ca[(UO_2)(PO_4)]_2(H_2O)_7$  (**Fig. 17**) [110].

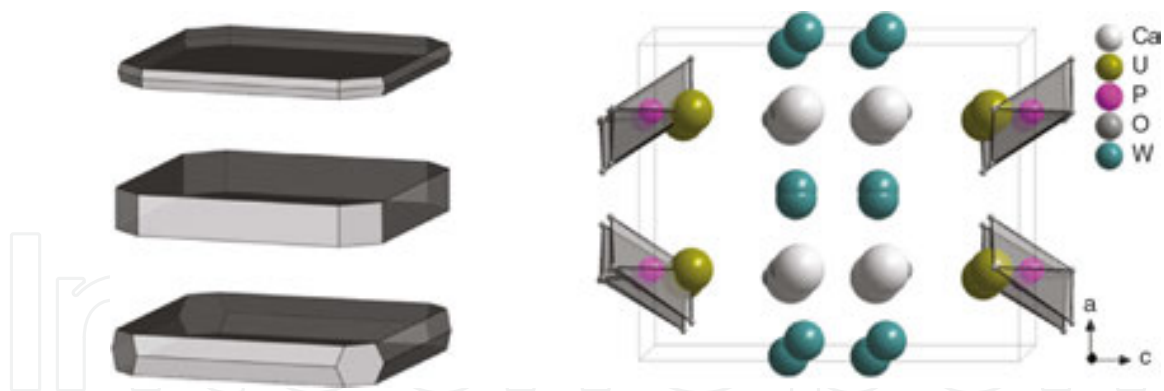


Fig. 17. The examples of forms and the structure of mineral meta-atunite [112] viewed along the b-axis.

2. **Crandallite** [113]:  $\text{CaAl}_3(\text{OH})_6[\text{PO}_3(\text{O}_{1/2}(\text{OH})_{1/2})_2]_2$ , has hexagonal structure ( $a = 7.005 \text{ \AA}$  and  $c = 16.192 \text{ \AA}$ ), which is analogous with alunite. The structure of mineral (Fig. 18) consists of corner-sharing Al octahedra, which are linked into trigonal and hexagonal rings to form the sheets perpendicular to the c-axis. Ca ions, surrounded by 12 oxygen and hydroxyl ions, lie in large cavities between the sheets. Each phosphate tetrahedron shares three corners with three Al octahedra from a trigonal ring in the sheet. The unshared corner is turned away from the trigonal hole towards the adjacent sheet to which it is hydrogen bonded. The mineral "deltaite" was found to be identical to crandallite, within the accuracy of the structural results.

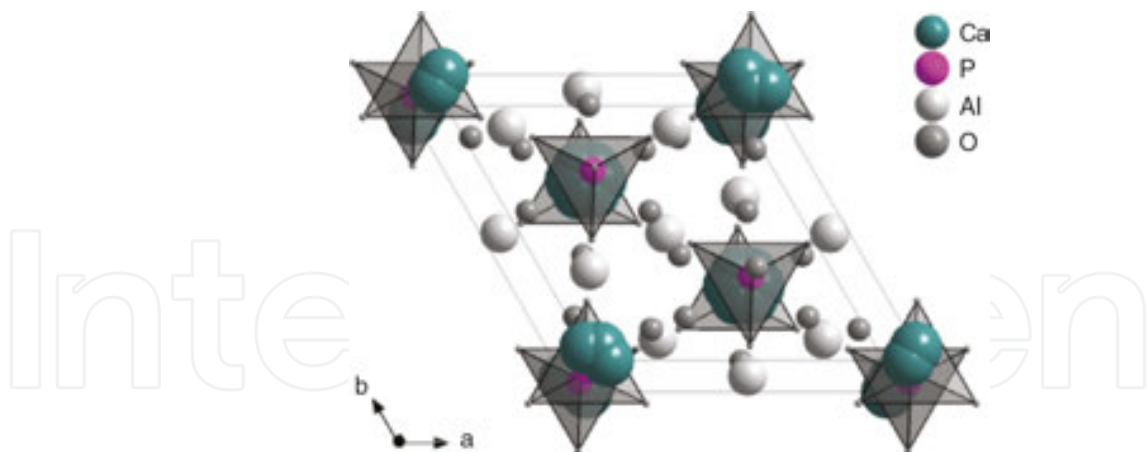
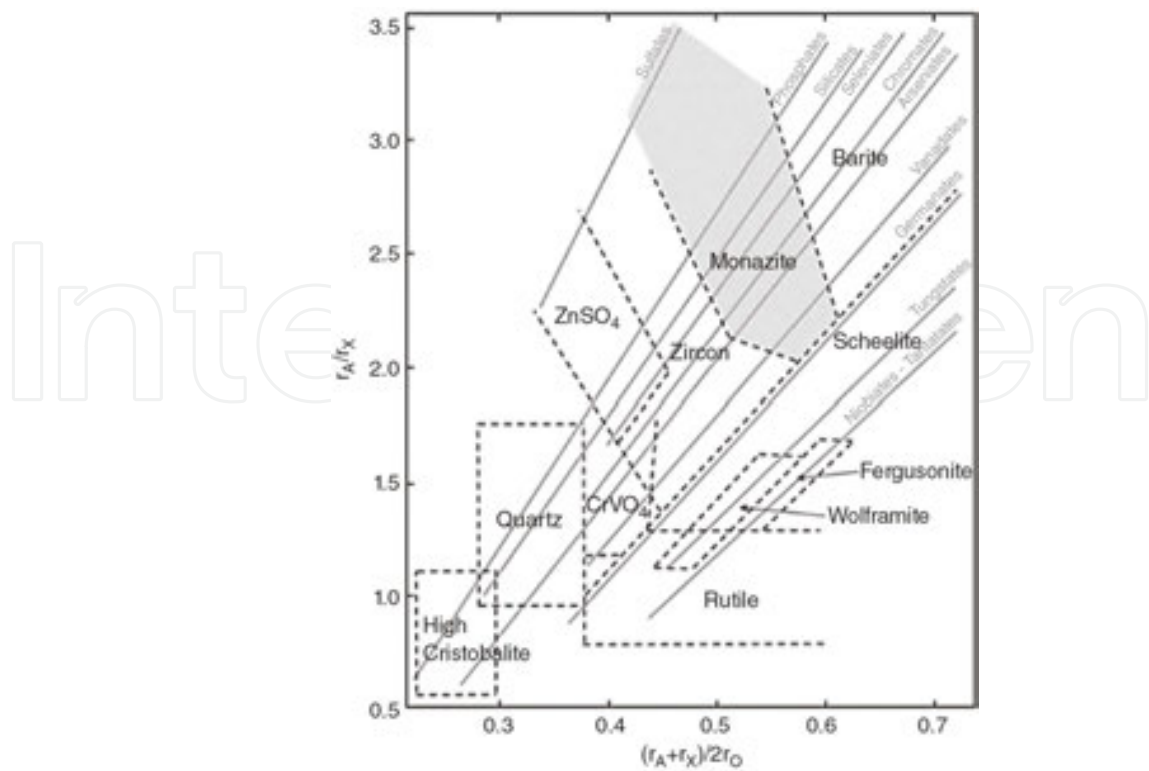


Fig. 18. The structure of mineral crandallite [113] viewed along the c-axis.

3. **Lazulite** [114],[115]: monoclinic mineral of the composition of  $\text{MgAl}_2(\text{PO}_4)_2(\text{OH})_2$ , which crystallizes in the  $P2_1/c$  space group and has the cell parameters:  $a = 7.16 \text{ \AA}$ ,  $b = 7.26 \text{ \AA}$  and  $c = 7.24 \text{ \AA}$  and  $\beta = 120.67^\circ$ . The mineral is the magnesium analogue of scorzalite ( $\text{Fe}^{2+}\text{Al}_2(\text{PO}_4)_2(\text{OH})_2$ ). Named in 1795 by MARTEN H. KLAPROTH from the Arabic word meaning "heaven," in allusion to its color.





**Fig. 21.** The classification diagram of  $AXO_4$ -type compounds. The monazite stability domain is colored by gray [117].

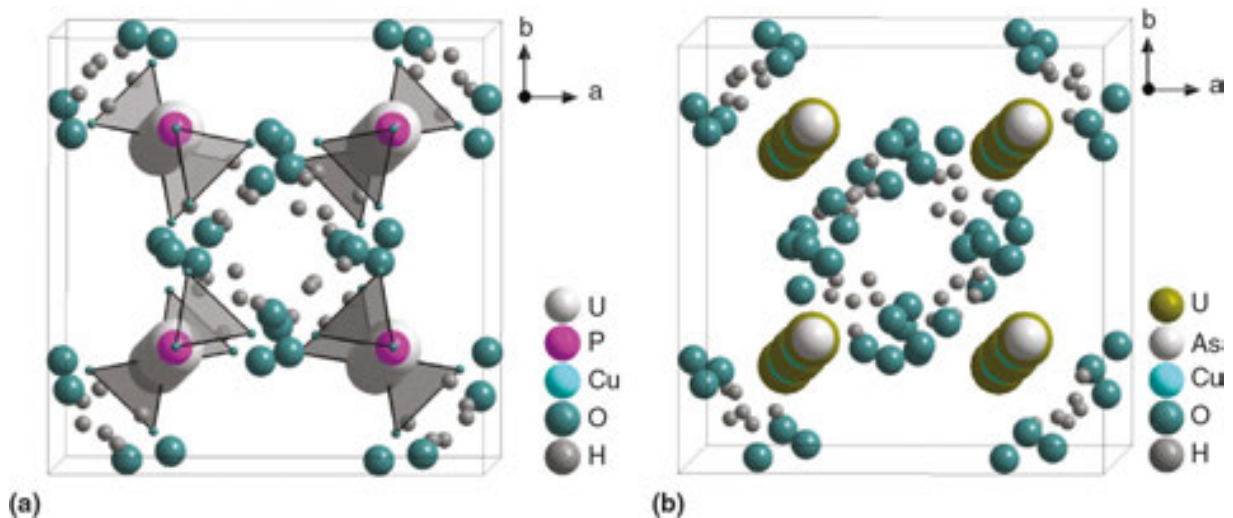


**Fig. 22.** The structure of tobernite and isostructural zeunerite [120] viewed along the  $c$ -axis.

- Tobernite** [120],[121]: tetragonal tobernite ( $P4/NNC$ ,  $a = 7.0267 \text{ \AA}$ ,  $c = 20.8070 \text{ \AA}$ ,  $c:a = 2.9611$ ,  $Cu[(UO_2)(PO_4)_2(H_2O)_{12}]$ , **Fig. 22(a)**) and zeunerite ( $Cu[(UO_2)(AsO_4)_2(H_2O)_{12}]$ , **Fig. 22(b)**), as well as metatorbernite ( $Cu[(UO_2)(PO_4)_2(H_2O)_8]$ ) and metazeunerite ( $Cu[(UO_2)(AsO_4)_2(H_2O)_8]$ ), belong to the autunite and meta-autunite groups, respectively, which

make up together approximately 40 mineral species of hydrated uranyl phosphates and arsenates. The structures, compositions and stabilities of minerals of the autunite and meta-autunite groups are of high interest because of their environmental significance. They are widespread and abundant and exert an impact on the mobility of uranium in phosphate-bearing systems and soils contaminated by actinides.

These minerals contain the autunite-type sheet, of the composition of  $[(\text{UO}_2)(\text{PO}_4)]^-$ , which involves the sharing of equatorial vertices of uranyl square bipyramids with phosphate tetrahedra. In each of these structures,  $\text{Cu}^{2+}$  cations are located between the sheets in Jahn-Teller<sup>32</sup> [122] distorted  $(4 + 2)$  octahedra, with short bonds to four  $\text{H}_2\text{O}$  groups in a square-planar arrangement and two longer distances to oxygen atoms of uranyl ions. A symmetrically independent  $\text{H}_2\text{O}$  group is held in each structure only by H-bonding, and in torbernite (and in zeunerite), it forms the square-planar sets of interstitial  $\text{H}_2\text{O}$  groups both above and below the planes of  $\text{Cu}^{2+}$  cations. In metatorbernite (and in metazeunerite), the square-planar sets of interstitial  $\text{H}_2\text{O}$  groups are either above or below the planes of  $\text{Cu}^{2+}$  cations. The bond-length-constrained refinement provides the crystal-chemically reasonable descriptions of H-bonding in those four structures [120].

7. **Turquoise** [123],[124]:  $\text{CuAl}_6(\text{PO}_4)_4(\text{OH})_8 \cdot 4\text{H}_2\text{O}$  is a copper analogue of triclinic mineral fausite  $\text{ZnAl}_6(\text{PO}_4)_4(\text{OH})_8 \cdot 4\text{H}_2\text{O}$  (the space group P1 with the cell parameters  $a = 7.410 \text{ \AA}$ ,  $b = 7.633 \text{ \AA}$ ,  $c = 9.904 \text{ \AA}$ ,  $\alpha = 68.4^\circ$ ,  $\beta = 69.65^\circ$  and  $\gamma = 65.05^\circ$ ). The structure (**Fig. 23**) consists of distorted  $\text{MO}_6$  polyhedra ( $M = \text{Zn}, \text{Cu}$ ),  $\text{AlO}_6$  octahedra and  $\text{PO}_4$  tetrahedra. By the edge- and corner-sharing of these polyhedra, a fairly dense three-dimensional framework is formed, which is further strengthened by a system of hydrogen bonds. The metal atoms in the unique  $\text{MO}_6$  ( $M = \text{Zn}$  or  $\text{Cu}$ ) polyhedron show a distorted  $[2 + 2 + 2]$  coordination, the distortion being more pronounced in turquoise. About 10% of the M site is vacant in both minerals. In turquoise, a previously undetected structural site with very low occupancy of (possibly) Cu is present at the position  $(1/2, 0, 1/2)$ .

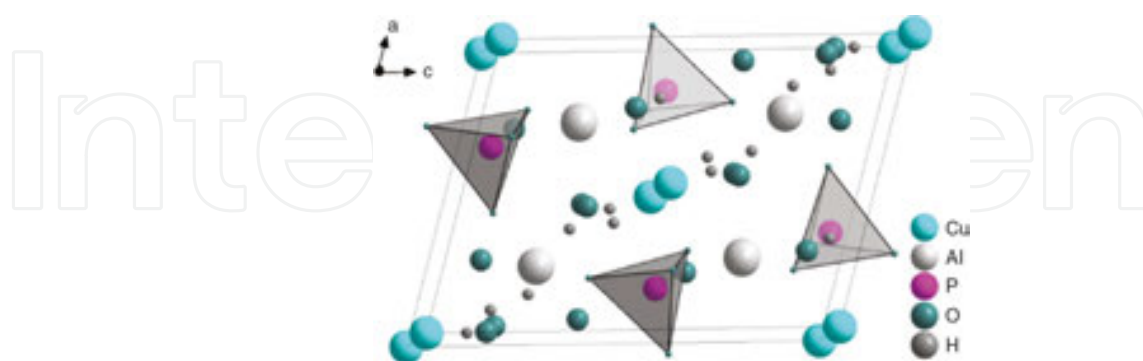


**Fig. 23.** The structure of turquoise viewed along the b-axis [124].

<sup>32</sup> According to the Jahn-Teller theorem, any nonlinear molecule in a degenerate electronic state will be unstable and will undergo some kind of distortion that will lower its symmetry so as to remove the degeneracy of the electronic state and also to attain lower energy. The Jahn-Teller effect is termed as static when there is permanent distortion in the structure of molecule [122].

8. **Vivianite** [125],[126],[127]: is monoclinic mineral of the composition of  $\text{Fe}_3(\text{PO}_4)_3 \cdot 8\text{H}_2\text{O}$ , which crystallizes in the space group of  $C1_2/M$  with the cell parameters  $a = 10.08 \text{ \AA}$ ,  $b = 13.43 \text{ \AA}$ ,  $c = 4.70 \text{ \AA}$  and  $\beta = 104.50^\circ$  (**Fig. 24**). The mineral was named by ABRAHAM GOTTLOB WERNER in 1817 after JOHN HENRY VIVIAN. Vivianite belongs to the simplest group of minerals with the composition given by general formula:  $\text{A}_3(\text{XO}_4)_2 \cdot 8\text{H}_2\text{O}$ , where A = Mg, Zn, Ni, Co or Fe and X is P or As [128].

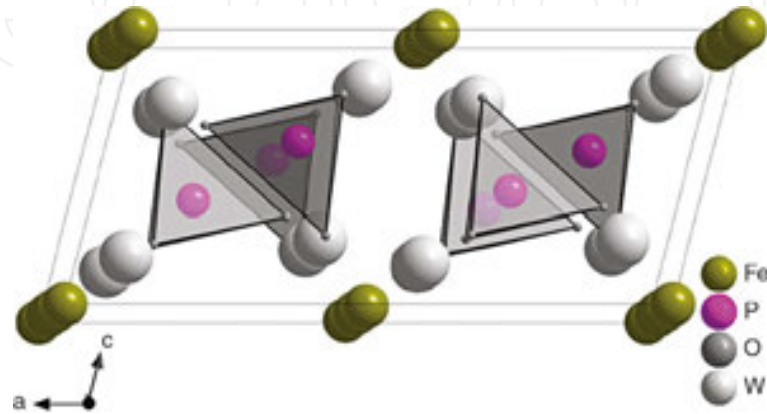


**Fig. 24.** The structure of vivianite viewed along the b-axis [125].

9. **Wavellite** [129]: the mineral of the composition of  $\text{Al}_3(\text{PO}_4)_2(\text{OH})_3 \cdot 4.5\text{--}5\text{H}_2\text{O}$  (the space group  $Pcmm$ ,  $a = 9.62 \text{ \AA}$ ,  $b = 17.36 \text{ \AA}$  and  $c = 6.99 \text{ \AA}$ ). The two aluminum atoms in the structure are octahedrally coordinated (**Fig. 25**): one is bonded to two O atoms, two  $-\text{OH}$  groups and two  $\text{H}_2\text{O}$  molecules and the other to three O, two  $(-\text{OH})$  and one  $\text{H}_2\text{O}$ . Phosphorus is in tetrahedral coordination with oxygen. Al octahedra, linked through (OH) corners, form chains parallel to the c-axis, and P tetrahedra are attached to this chain by sharing O atoms of subsequent octahedra. An extra  $\text{H}_2\text{O}$  molecule occupies the large cavity between the chains, and as indicated by a high temperature factor, it has a statistical distribution within this cavity.

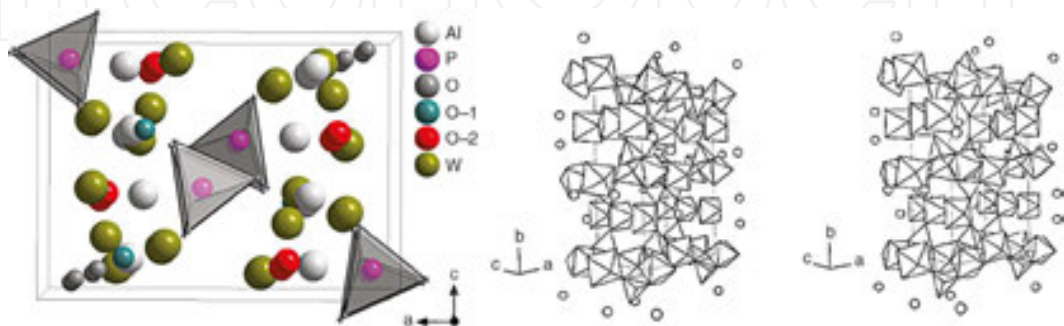


**Fig. 25.** The structure of wavellite viewed along the b-axis (a) and stereoscopic view of the wavellite structure (b) [129].

**10. Xenotime** [118]: monazite (**Fig. 26**) is isostructural with zircon ( $I4_1/AMD$ ). Monazite atomic arrangement as well as that of xenotime is based on [001] chains of intervening phosphate tetrahedra and RE polyhedra, with REO, polyhedron in xenotime that accommodates heavy lanthanides (Tb-Lu in the synthetic phases) and REO polyhedron in monazite that preferentially incorporates larger light rare-earth elements (La-Gd). As the structure “transforms” from xenotime to monazite, the crystallographic properties are comparable along the [001] chains, with the structural adjustments to the different sizes of REE atoms occurring principally in (001).

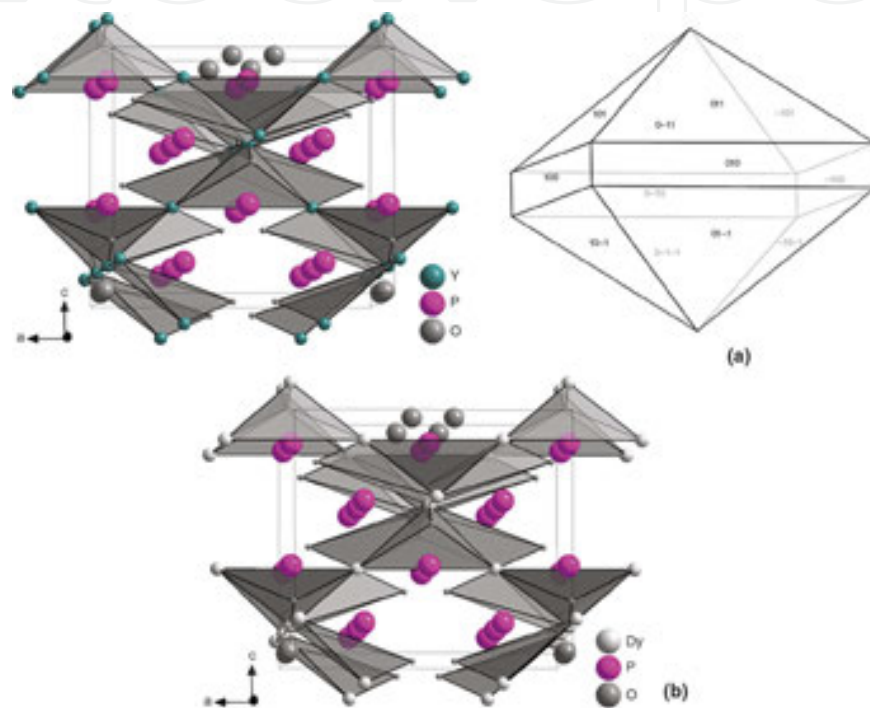


**Fig. 26.** The structure of xenotime-(Y):  $a = 6.8947 \text{ \AA}$ ,  $b = 6.8947 \text{ \AA}$  and  $c = 6.0276 \text{ \AA}$  (a) and xenotime-(Dy) (b)  $a = 6.9052 \text{ \AA}$ ,  $b = 6.9053 \text{ \AA}$  and  $c = 6.0384 \text{ \AA}$  (b) [118] viewed along the b-axis.

Isostructural arsenate analogues of many phosphate minerals are known, and in some cases, vanadates too. Some orthophosphates capable of forming complete ranges of solid solutions with the corresponding orthoarsenates are [25]:

- **Variscite group:**  $MXO_4 \cdot 2H_2O$ , where  $M = Fe, Al$  and  $X = P$  or  $As$ ;
- **Fairfieldite group:**  $Ca_2M(XO_4)_2 \cdot 2H_2O$ , where  $M = Mn, Fe, Mg, Ni, Zn, Co$  and  $X = P, As$ ;
- **Vivianite group:**  $M_3(XO_4)_2 \cdot 8H_2O$ , where  $M = Fe, Mn, Mg, Zn, Co, Ni$  and  $X = P, As$ ;
- **Monazite group:**  $MXO_4$ , where  $M = Ce, La, Nd, Th, Bi$  and  $X = P, As$ ;
- **Rhabdophane group:**  $MXO_4 \cdot H_2O$ , where  $M = Ce, La, Nd, Th$  and  $X = P, As$ ;
- **Xenotime group:**  $MXO_4$ , where  $M = Y, Ce, Bi$  and  $X = P, V$ ;

- **Autunite group:**  $M[(\text{UO}_2)_2(\text{XO}_4)] \cdot n\text{H}_2\text{O}$ , where  $M = \text{Ca, Ce, Ba, K, NH}_4^+, \text{Sr, Pb, Mg, Na, Zn}$  and  $X = \text{P, As, V}$ ;
- **Crandallite group:**  $\text{MM}'_3(\text{XO}_4)_2(\text{OH})_6 \cdot \text{H}_2\text{O}$ , where  $M = \text{Ca, Sr, Ba}$ ,  $M' = \text{Al, Fe}$  and  $X = \text{P, As}$ .

Phosphate minerals, like silicate minerals, are found with a great variety of cations. Unlike the latter group that contains numerous types of condensed silicate anions, almost all phosphate minerals are orthophosphates that contain  $\text{PO}_4^{3-}$  anion. Non-phosphorus anions, such as  $\text{O}^{2-}$ ,  $\text{OH}^-$ ,  $\text{F}^-$ ,  $\text{Cl}^-$ ,  $\text{SO}_4^{2-}$ ,  $\text{SiO}_4^{4-}$  and  $\text{AsO}_4^{3-}$ , may also be present in these stoichiometric (or as occluded) materials [25].

## Author details

Petr Ptáček

Brno University of Technology, Czech Republic

## References

- [1] Bishop AC, Woolley AR, Woolley WRH. Cambridge Guide to Minerals, Rocks and Fossils. 2nd ed., Cambridge: Cambridge University Press, 1999. ISBN: 0-521-77881-6
- [2] Clarke FW. The Data of Geochemistry. Bulletin (Geological Survey (U.S.)), U.S. Government Printing Office, 1920.
- [3] McClellan GH, Lehr JR. Crystal chemical investigation of natural apatites. American Mineralogist 1969;54 1374–1391.
- [4] Ding T, Ma D, Lu J, Zhang R. Apatite in granitoids related to polymetallic mineral deposits in southeastern Hunan Province, Shi-Hang Zone, China: Implications for petrogenesis and metallogenesis. Ore Geology Reviews 2015;69 104–117.
- [5] Watson EB. Apatite and phosphorus in mantle source regions: an experimental study of apatite/melt equilibria at pressures to 25 kbar. Earth and Planetary Science Letters 1980;51(2) 322–335.
- [6] Deer WA. Rock-Forming Minerals: Non-silicates. Volume 5B, 2nd ed., Geological Society of London, 1998. ISBN: 978-1897799901
- [7] Raask E. Mineral Impurities in Coal Combustion: Behavior, Problems, and Remedial Measures. Taylor & Francis, 1985. ISBN: 978-3540138174
- [8] Jacobson M, Charlson RJ, Rodhe H, Orians GH. Earth System Science: From Biogeochemical Cycles to Global Changes. International Geophysics — Volume 72. Academic Press, 2000. ISBN: 978-0080530642

- [9] Spear FS. *Metamorphic Phase Equilibria and Pressure-Temperature-Time Paths*. Mineralogical Society of America short course notes. 2nd ed., Mineralogical Society of America, 1993. ISBN: 978-0939950348
- [10] Kemp JF. *A Handbook of Rocks for Use Without the Microscope*. BiblioBazaar, 2009. ISBN: 978-1110466528
- [11] Drouet Ch. A comprehensive guide to experimental and predicted thermodynamic properties of phosphate apatite minerals in view of applicative purposes. *Journal of Chemical Thermodynamics* 2015;81 143–159.
- [12] Ihlen PM, Schiellerup H, Gautneb H, Skår Ø. Characterization of apatite resources in Norway and their REE potential — A review. *Ore Geology Reviews* 2014;58 126–147.
- [13] Santana RC, Farnese ACC, Fortes MCB, Ataíde CH, Barrozo MAS. Influence of particle size and reagent dosage on the performance of apatite flotation. *Separation and Purification Technology* 2008;64(1) 8–15.
- [14] Pucéat E, Reynard B, Lécuyer C. Can crystallinity be used to determine the degree of chemical alteration of biogenic apatites? *Chemical Geology* 2004;205(1-2) 83–97.
- [15] Zafar ZI, Anwar MM, Pritchard DW. Optimization of thermal beneficiation of a low grade dolomitic phosphate rock. *International Journal of Mineral Processing* 1995;43(1-2) 123–131.
- [16] dos Santos MA, Santana RC, Capponi F, Ataíde CH, Barrozo MAS. Effect of ionic species on the performance of apatite flotation. *Separation and Purification Technology* 2010;76(1) 15–20.
- [17] Chen M, Graedel TE. The potential for mining trace elements from phosphate rock. *Journal of Cleaner Production* 2015;91 337–346.
- [18] Al-Bassam KS, Aba-Hussain AA, Mohamed IQ, Al-Rawi Yehya T. Petrographic classification of phosphate components of East Mediterranean phosphorite deposits. *Iraqi Bulletin of Geology and Mining* 2010;6(1) 59–79.
- [19] Flügel E. *Microfacies of Carbonate Rocks: Analysis, Interpretation and Application*. Springer Science & Business Media, 2013. ISBN: 978-3662087268
- [20] Abouzeid A-ZM. Physical and thermal treatment of phosphate ores — An overview. *International Journal of Mineral Processing* 2008;85(4) 59–84.
- [21] Gupta AK. *Igneous Rocks*. Allied Publishers, 1998. ISBN: 978-8170237846
- [22] *Manual Fertilizer*, UN Industrial Development Organization, International Fertilizer Development Center. Springer Science & Business Media, 1998. ISBN: 978-0792350323
- [23] *World Phosphate Rock Reserves and Resources*. International Center for Soil Fertility and Agricultural Development, 2010. ISBN: 978-0880901673
- [24] Emich GD. Phosphate rock. *Industrial Minerals and Rocks* 1984;2 1017–1047.

- [25] Derek EC. *Chemistry, Biochemistry and Technology*. 6th ed., CRC Press, 2013. ISBN: 978-1439840887
- [26] Teleki PG, Dobson MR, Moore JR, von Stackelberg U. *Marine Minerals: Advances in Research and Resource Assessment*. Nato Science Series C: Volume 194. Springer Science & Business Media, 2012. ISBN: 978-9400938038
- [27] McKelvey VE. *Phosphate Deposits*. Geological Survey Bulletin 1252-D. A Summary of Salient Features of the Geology of Phosphate Deposits, Their Origin, and Distribution. Washington: United States Government Printing Office, 1967.
- [28] Cook PJ, Shergold JH. *Phosphate Deposits of the World: Volume 1: Proterozoic and Cambrian Phosphorites*. Cambridge Earth Science Series. Cambridge University Press, 2005. ISBN: 978-0521619219
- [29] Salvador A. *International Stratigraphic Guide: A Guide to Stratigraphic Classification, Terminology, and Procedure*. Publication (International Union of Geological Sciences). 30th ed., Geological Society of America, 1994. ISBN: 978-0813774015
- [30] Walter MR. *Stromatolites*. *Developments in Sedimentology*. Elsevier, 1976. ISBN: 978-0080869322
- [31] Nairn AEM, Ricou Luc-E, Vrielynck B, Dercourt J. *The Tethys Ocean*. *Ocean Basins and Margins – Volume 8*. Springer Science & Business Media, 2013. ISBN: 978-1489915580
- [32] Notholt AJG, Sheldon RP, Davidson DF. *Phosphate Deposits of the World: Volume 2, Phosphate Rock Resources*. Cambridge Earth Science Series. Revised edition, Cambridge University Press, 2005. ISBN: 978-0521673334
- [33] Gualtieri A, Venturelli P. In situ study of the goethite-hematite phase transformation by real time, synchrotron powder diffraction, sample at T = 25 C. *American Mineralogist* 1999;84 895–904.
- [34] Nathan Y. Phosphate minerals. In: Nriagu JO, Moore PB (Eds.), Chapter 8. *The Mineralogy and Geochemistry of Phosphorites*. Springer Science & Business Media, 2012. ISBN: 978-3642617362
- [35] Rao VP. Phosphorites from the Error Seamount, northern Arabian Sea. *Marine Geology* 1986;71(1-2) 177–186.
- [36] Glenn CR, Föllmi KB, Riggs SR, Baturin GN, Grimm KA, Trape J. Phosphorus and phosphorites: Sedimentology and environments of formation. *Eclogae Geologicae Helvetiae* 1994;87(3) 747–788.
- [37] Baturin GN, Bezrukov PL. Phosphorites on the sea floor and their origin. *Marine Geology* 1979;31(3-4) 317–332.
- [38] Cook PJ, Shergold JH, Burnett WC, Riggs SR. *Phosphorite research: A historical overview*. Geological Society, London, Special Publications 1990;52 1–22.

- [39] Trappe J. Phanerozoic Phosphorite Depositional Systems: A Dynamic Model for a Sedimentary Resource System. Lecture Notes in Earth Sciences — Volume 76, ISSN 0930-0317. Springer, 1998. ISBN: 978-3540696049
- [40] Bogdanov NA. Non-metallic Mineral Ores. Proceedings of the 27th International Geological Congress — Volume 15. VSP, 1984. ISBN: 978-9067640244
- [41] Dunham RJ. Classification of carbonate rocks according to depositional texture, in: Ham WE. Classification of carbonate rocks. American Association of Petroleum Geologists Memoir 1962;1 108–121.
- [42] Riggs SR. A petrographic classification of sedimentary phosphorites. In: Cook PJ, Shergold JH. (Eds.), Proterozoic–Cambrian Phosphorites. IGCP, 156, 1st Field Workshop and Seminar. Canberra: National Library of Australia, 1979.
- [43] Suess E, von Huene R. Proceedings of the Ocean Drilling Program, Scientific Results, Volume 112. Phosphatic Sediments and Rocks Recovered from the Peru Margin during ODP LEG 1121. The Program, 1986.
- [44] Ehrlich HL, Newman DK. Geomicrobiology. 5th ed., CRC Press, 2008. ISBN: 978-0849379079
- [45] Tyrrell GW. The Principles of Petrology: An Introduction to the Science of Rocks. Springer Science & Business Media, 2012. ISBN: 978-9401160261
- [46] Gill R. Igneous Rocks and Processes: A Practical Guide. John Wiley & Sons, 2011. ISBN: 978-1444362435
- [47] Brown PW, Constanz B. Hydroxyapatite and Related Materials. CRC Press, 1994. ISBN: 978-0849347504
- [48] Wenk Hans-R, Bulakh A. Minerals: Their Constitution and Origin. Cambridge University Press, 2004. ISBN: 978-0521529587
- [49] Laenen B, Hertogen J, Vandenberghe N. The variation of the trace-element content of fossil biogenic apatite through eustatic sea-level cycles. *Palaeogeography, Palaeoclimatology, Palaeoecology* 1997;132(1-4) 325–342.
- [50] Egorov LS. Ijolite-Carbonatite Plutonism (in Russian). Nedra, Leningrad, 1991.
- [51] Isakova AT, Panina LI, Rokosova EY. Carbonatite melts and genesis of apatite mineralization in the Guli pluton (northern East Siberia). *Russian Geology and Geophysics* 2015;56(3) 466–475.
- [52] Dawson JB, Steele IM, Smith JV, Rivers ML. Minor and trace element chemistry of carbonates, apatites and magnetites in some African carbonatites. *Mineralogical Magazine* 1996;60 415–425.
- [53] Aspden JA. The mineralogy of primary inclusions in apatite crystals extracted from Alnö ijolite. *Lithos* 1980;13(3) 263–268.

- [54] Cordeiro PFO, Brod JA, Dantas EL, Barbosa ESR. Mineral chemistry, isotope geochemistry and petrogenesis of niobium-rich rocks from the Catalão I carbonatite-phoscorite complex, Central Brazil. *Lithos* 2010;118(3-4) 223–237.
- [55] Iddings JP. *Igneous Rocks: Composition, Texture and Classification, Description and Occurrence, Volume 1*. Рипол Классик, 1920. ISBN: 978-5883586766
- [56] Wall F, Zaitsev AN. *Phoscorites and Carbonatites from Mantle to Mine: The Key Example of the Kola Alkaline Province*. Mineralogical Society of Great Britain & Ireland, 2004. ISBN: 978-0903056229
- [57] Russell HD, Hiemstra SA, Groeneveld D. New aspects of the Lower Katanga rocks of the Kafue Gorge. *Transactions of the Geological Society of South Africa* 1955;58 197–208.
- [58] Le Maitre RW, Streckeisen A, Zanettin B, Le Bas MJ, Bonin B, Bateman P. *Igneous Rocks: A Classification and Glossary of Terms: Recommendations of the International Union of Geological Sciences Subcommittee on the Systematics of Igneous Rocks*. 2nd ed., Cambridge University Press, 2002. ISBN: 978-1139439398
- [59] *Reviews Book: Igneous Rocks: A Classification and Glossary of Terms (Recommendations of the IUGS Subcommittee on the Systematics of Igneous Rocks)*. 2nd ed., LeMaitre RW (ed.). Cambridge University Press, New York, N.Y., 2002. ISBN: 0-521-66215-X. *The Canadian Mineralogist* 2002;40 1737-1742.
- [60] Kucera M. *Industrial Minerals and Rocks: Developments in Economic Geology*. Elsevier, 2013. ISBN: 978-0444597502
- [61] Tatarinov PM. *Nonmetallic mineral deposits course (in Russian)*. Moscow: Nedra, 1969.
- [62] Wills BA. *Mineral Processing Technology: An Introduction to the Practical Aspects of Ore Treatment and Mineral Recovery (in SI/Metric Units)*. International Series on Materials Science and Technology. 4th ed., Elsevier, 2013. ISBN: 978-483286679
- [63] Iijima A, Abed AM. Siliceous, Phosphatic and Clauconitic Sediments of the Tertiary and Mesozoic. *Proceedings of the 29th International Geological Congress: Kyoto, Japan, 24 August-3 September 1992 – Part 3*. VSP, 1994. ISBN: 978-9067641753
- [64] Cronan DS. *Marine Minerals in Exclusive Economic Zones. Topics in the Earth Sciences – Volume 5*. Springer Science & Business Media, 1992. ISBN: 978-0412292705
- [65] Cushman GT. *Guano and the Opening of the Pacific World: A Global Ecological History*. Studies in Environment and History. Cambridge University Press, 2013. ISBN: 978-1107004139
- [66] Hollett D. *More Precious Than Gold: The Story of the Peruvian Guano Trade*. Associated University Press, 2008. ISBN: 978-0838641316
- [67] Chang Jen-S, Kelly A, Crowley JM. *Handbook of Electrostatic Processes*. CRC Press, 1995. ISBN: 978-1420066166

- [68] Nogalska A, Zalewska M. The effect of meat and bone meal on phosphorus concentrations in soil and crop plants. *Plant Soil Environment* 2013;59(12) 575–580.
- [69] O'Reilly SY, Griffin WL. Apatite in the mantle: implications for metasomatic processes and high heat production in Phanerozoic mantle. *Lithos* 2000;53 217–232.
- [70] Douce AEP, Roden MF, Chaumba J, Fleisher C, Yogodzinski G. Compositional variability of terrestrial mantle apatites, thermodynamic modeling of apatite volatile contents, and the halogen and water budgets of planetary mantles. *Chemical Geology* 2011;288 14–31.
- [71] Sha LK, Chappell BW. Apatite chemical composition, determined by electron microprobe and laser-ablation inductively coupled plasma mass spectrometry, as a probe into granite petrogenesis. *Geochimica et Cosmochimica Acta* 1999;63(22) 3861–3881.
- [72] Joosu L, Lepland A, Kirsimäe K, Romashkin AE, Roberts NMW, Martin AP, Črne AE. The REE-composition and petrography of apatite in 2 Ga Zaonega Formation, Russia: The environmental setting for phosphogenesis. *Chemical Geology* 2015;395 88–107.
- [73] Föllmi KB. The phosphorus cycle, phosphogenesis and marine phosphate-rich deposits. *Earth-Science Reviews* 1996;40(1-2) 55–124.
- [74] Glenn CR, Föllmi KB, Riggs Sr, Baturin GN, Grimm KA, Trappe J. Phosphorus and phosphorites: sedimentology and environments of formation. *Eclogae Geologicae Helvetiae* 1994;87(3) 747–788.
- [75] Jarvis I, Burnett WC, Nathan Y, Almbaydin FSM, Attia AKM, Castro LN, Flicoteaux R, Hilmy ME, Husain V, Qutawnah AA, Serjani A, Zanin YN. Phosphorite geochemistry – State-of-the-art and environmental concerns. *Eclogae Geologicae Helvetiae* 1994;87(3) 643–700.
- [76] Alexander EB. *Soils in Natural Landscapes*. CRC Press, 2013. ISBN: 978-1466594364
- [77] Jørgensen SE. *Global Ecology*. Academic Press, 2010. ISBN: 978-0444536273
- [78] CIBA Foundation Symposium. *Phosphorus in the Environment: Its Chemistry and Biochemistry*. Novartis Foundation Symposia – Volume 919. John Wiley & Sons, 2009. ISBN: 978-0470718070
- [79] Ragot S, Zeyer J, Zehnder L, Reusser E, Brandl H, Lazzaro A. Bacterial community structures of an alpine apatite deposit. *Geoderma* 2013;202-203 30-37.
- [80] Puente ME, Rodriguez-Jaramillo MC, Li CY, Bashan Y. Image analysis for quantification of bacterial rock weathering. *Journal of Microbiological Methods* 2006;64(2) 275–286.
- [81] Nies A. Strengit, ein neues Mineral. *Neues Jahrbuch für Mineralogie, Geologie und Palaontologie* 1877; 8-16.
- [82] Cornelis P. *Pseudomonas: Genomics and Molecular Biology*. Horizon Scientific Press, 2008. ISBN: 978-1904455196

- [83] Pongslip N. Phenotypic and Genotypic Diversity of Rhizobia. Bentham Science Publishers, 2012. ISBN: 978-1608054619
- [84] Vanlaere E. *Burkholderia cepacia* complex. DCL Print & Sign, 2008. ISBN: 978-9087560379
- [85] Lisker F, Ventura B, Glasmacher UA. Apatite thermochronology in modern geology. Geological Society, London, Special Publications 2009;324 1–23. DOI: 10.1144/SP324.1.
- [86] Fleischer RL, Price PB, Walker RM. Nuclear Tracks in Solids: Principles and Applications. University of California Press, 1975. ISBN: 978-0520026650
- [87] Fleisher RL, Price PB. Techniques for geological dating of minerals by chemical etching of fission fragment tracks. *Geochimica et Cosmochimica Acta* 1964;28(11) 1705–1714.
- [88] Galbraith RF. Statistics for Fission Track Analysis. CRC Press, 2005. ISBN: 978-1420034929
- [89] Li W, Wang L, Lang M, Trautmann C, Ewing RC. Thermal annealing mechanisms of latent fission tracks: Apatite vs. zircon. *Earth and Planetary Science Letters* 2011;302(1-2) 227–235.
- [90] Li W, Lang M, Gleadow AJW, Zdorovets MV, Ewing RC. Thermal annealing of unetched fission tracks in apatite. *Earth and Planetary Science Letters* 2012;321-322 121-127.
- [91] Chen H, Hu J, Wu G, Shi W, Geng Y, Qu H. Apatite fission-track thermochronological constraints on the pattern of late Mesozoic-Cenozoic uplift and exhumation of the Qinling Orogen, central China. *Journal of Asian Earth Sciences* 2014. In press. DOI: 10.1016/j.jseas.2014.10.004.
- [92] Hejl E. Evidence for unetchable gaps in apatite fission tracks. *Chemical Geology* 1995;122(1-4) 259–269.
- [93] Peternell M, Kohlmann F, Wilson CJL, Seiler C, Gleadow AJW. A new approach to crystallographic orientation measurement for apatite fission track analysis: Effects of crystal morphology and implications for automation. *Chemical Geology* 2009;265(3-4) 527–539.
- [94] Enkelmann E, Ehlers TA, Buck G, Schatz Ann-K. Advantages and challenges of automated apatite fission track counting. *Chemical Geology* 2012;322-323 278-289.
- [95] van den Haute P, De Corte F. *Advances in Fission-Track Geochronology*. Solid Earth Sciences Library – Volume 10. Springer Science & Business Media, 2013. ISBN: 978-9401591331
- [96] McCubbin FM, Jolliff BL, Nekvasil H, Carpenter PK, Zeigler RA, Steele A, Elardo SM, Lindsley DH. Fluorine and chlorine abundances in lunar apatite: Implications for heterogeneous distributions of magmatic volatiles in the lunar interior. *Geochimica et Cosmochimica Acta* 2011;75(17) 5073–5093.
- [97] Boyce JW, Tomlinson SM, McCubbin FM, Greenwood JP, Treiman AH. The lunar apatite paradox. *Science* 25;344(6182) 400-402.

- [98] Crotts APS. Lunar outgassing, transient phenomena, and the return to the Moon. Part 1: Existing data. *The Astrophysical Journal* 2008;687 692–705.
- [99] Calvo C, Gopal R. The crystal structure of whitlockite from the Palermo quarry. *American Mineralogist* 1975;60 120–133.
- [100] McConnell D. *Apatite: Its Crystal Chemistry, Mineralogy, Utilization, and Geologic and Biologic Occurrences: Applied Mineralogy (Volume 5)*. Springer Science & Business Media, 2012. ISBN: 978-3709183144
- [101] Jolliff BL, Hughes JM, Freeman JJ, Zeigler RA. Crystal chemistry of lunar merrillite and comparison to other meteoritic and planetary suites of whitlockite and merrillite. *American Mineralogist* 2006;91 1583–1595. DOI: 10.2138/am.2006.2185 1583.
- [102] Hughes JM, Jolliff BL, Gunter ME. The atomic arrangement of merrillite from the Fra Mauro Formation, Apollo 14 lunar mission: The first structure of merrillite from the Moon. *American Mineralogist* 2006;91 1547–1552.
- [103] Barnes JJ, Tartèse R, Anand M, McCubbin FM, Franchi IA, Starkey NA, Russell SS. The origin of water in the primitive Moon as revealed by the lunar highlands samples. *Earth and Planetary Science Letters* 2014;390 244–252.
- [104] Douce AEP, Roden M. Apatite as a probe of halogen and water fugacities in the terrestrial planets. *Geochimica et Cosmochimica Acta* 2006;70(12) 3173–3196.
- [105] Hallis LJ, Taylor GJ, Nagashima K, Huss GR. Magmatic water in the Martian meteorite Nakhla. *Earth and Planetary Science Letters* 2012;359-360 84-92.
- [106] Sarafian AR, Roden MF, Patiño-Douce AE. The volatile content of Vesta: Clues from apatite in eucrites. *Meteoritics & Planetary Science* 2013,48(11) 2135–2154.
- [107] Scully JEC, Russell CT, Yin A, Jaumann R, Carey E, Castillo-Rogez J, McSween HY, Raymond CA, Reddy V, Le Corre L. Geomorphological evidence for transient water flow on Vesta. *Earth and Planetary Science Letters* 2015;411 151–163.
- [108] Treiman AH, Lanzirotti A, Xirouchakis D. Ancient water on asteroid 4 Vesta: evidence from a quartz veinlet in the Serra de Magé eucrite meteorite. *Earth and Planetary Science Letters* 2004;219(3-4) 189–199.
- [109] Jasinski SM. Phosphate rock. U.S. Geological Survey Mineral Commodity Summaries 2007; 120-121.
- [110] Locock AJ, Burns PC. The crystal structure of synthetic autunite,  $\text{Ca}[(\text{UO}_2)(\text{PO}_4)]_2(\text{H}_2\text{O})_{11}$ . *American Mineralogist* 2003;88 240–244.
- [111] Phillips W, Brooke HJ, Miller WH. Autunite. In: *An Elementary Introduction to Mineralogy*. London: Longman, Brown, Green, and Longman, 1852; 519-519.
- [112] Makarov ES, Ivanov VI. The crystal structure of meta-autunite,  $\text{Ca}(\text{UO}_2)_2(\text{PO}_4)_2 \cdot 6\text{H}_2\text{O}$ . *Doklady Akademii Nauk SSSR* 1960;132 601–603.
- [113] Blount AM. The crystal structure of crandallite. *American Mineralogist* 1974;59 41–47.

- [114] Lindberg ML, Christ CL. Crystal structures of the isostructural minerals lazulite, scorzalite and barbosalite. *Acta Crystallographica* 1959;12 695–697.
- [115] Giuseppetti G, Tadini C. Lazulite,  $(\text{Mg,Fe})\text{Al}_2(\text{OH})_2(\text{PO}_4)_2$ : structure refinement and hydrogen bonding. *Neues Jahrbuch fur Mineralogie, Monatshefte* 1983; 410-416.
- [116] Larsen ES, Shannon EV. The minerals of the phosphate nodules from near Fairfield, Utah. *American Mineralogist* 1930;15 307–337.
- [117] Clavier N, Podor R, Dacheux N. Crystal chemistry of the monazite structure. *Journal of the European Ceramic Society* 2011;31(6) 941–976.
- [118] Ni Y, Hughes JM, Mariano AN. Crystal chemistry of the monazite and xenotime structures. *American Mineralogist* 1995;80 21–26.
- [119] Rutley F. *Mineralogy Murby's "Science and Art Department" series of textbooks*. Thomas Murby & Company, 1802.
- [120] Locock AJ, Burns PC. Crystal structures and synthesis of the copper-dominant members of the autunite and meta-autunite groups: Torbernite, zeunerite, metatorbernite and metazeunerite. *The Canadian Mineralogist* 2003;41 489–502.
- [121] Hennig C, Reck G, Reich T, Robberg A, Kraus W, Sieler J. EXAFS and XRD investigations of zeunerite and meta-zeunerite. *Zeitschrift fur Kristallographie* 2003;218 37–45.
- [122] Sathyanarayana DN. *Electronic Absorption Spectroscopy and Related Techniques*. Universities Press, 2001. ISBN: 978-8173713712
- [123] Cid-Dresdner H. Determination and refinement of the crystal structure of turquoise,  $\text{CuAl}_6(\text{PO}_4)_4(\text{OH})_8 \cdot 4\text{H}_2\text{O}$ . *Zeitschrift fur Kristallographie* 1965;121 87–113.
- [124] Kolitsch U, Giester G. The crystal structure of faustite and its copper analogue turquoise. *Mineralogical Magazine* 2000;64 905–913.
- [125] Werner AG. Vivianit, in *Letztes Mineral-System, bey Craz und Gerlach, und bey Carl Gerold* (Freiberg und Wien) 1817; 41-42.
- [126] Fejdi P, Poullen JF, Gasperin M. Affinement de la structure de la vivianite  $\text{Fe}_3(\text{PO}_4)_2 \cdot 8\text{H}_2\text{O}$ . *Bulletin de Mineralogie* 1980;103 135–138.
- [127] Bartl H. Water of crystallization and its hydrogen-bonded crosslinking in vivianite  $\text{Fe}_3(\text{PO}_4)_2 \cdot 8\text{H}_2\text{O}$ ; a neutron diffraction investigation. *Zeitschrift fur Analytische Chemie* 1989;333 401–403.
- [128] Mori H, Ito T. The structure of vivianite and symplecite. *Acta Crystallographica* 1950;3 1–6.
- [129] Araki T, Zoltai T. The crystal structure of wavellite. *Zeitschrift fur Kristallographie* 1968;127 21–33.

